Synthesis Y. Wei et al. Review

Visible-Light-Driven Organic Photochemical Reactions in the Absence of External Photocatalysts

Yi Wei[a]
Quan-Quan Zhou[a]
Fen Tan*[b]
Liang-Qiu Lu*[a]
Wen-Jing Xiao[a]

[a] CCNU-uOttawa Joint Research Centre, Key Laboratory of Pesticide & Chemical Biology, Ministry of Education, College of Chemistry, Central China Normal University, 152 Luoyu Road, Wuhan, Hubei, 430079, P. R. of China
luliangqiu@mail.ccnu.edu.cn
[b] Hubei Key Laboratory of Purification and Application of Plant Anti-cancer Active Ingredients, Hubei University of Education, Wuhan, Hubei, 430205, P. R. of China
tanfen@hue.edu.cn

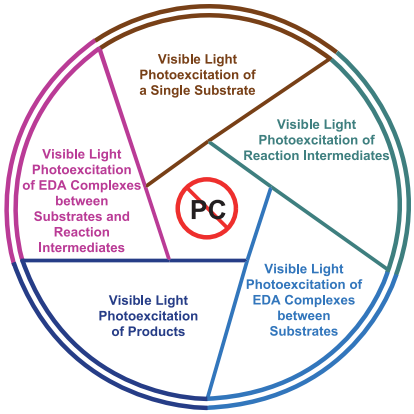

Received: 22.02.2019
Accepted after revision: 25.03.2019
Published online: 20.05.2019
DOI: 10.1055/s-0037-1611812; Art ID: ss-2019-e0116-r

Abstract Visible-light-driven organic photochemical reactions have attracted substantial attention from the synthetic community. Typically, catalytic quantities of photosensitizers, such as transition metal complexes, organic dyes, or inorganic semiconductors, are necessary to absorb visible light and trigger subsequent organic transformations. Recently, in contrast to these photocatalytic processes, a variety of photocatalyst-free organic photochemical transformations have been exploited for the efficient formation of carbon–carbon and carbon–heteroatom bonds. In addition to not requiring additional photocatalysts, they employ low-energy visible light irradiation, have mild reaction conditions, and enable broad substrate diversity and functional group tolerance. This review will focus on a summary of representative work in this field in terms of different photoexcitation modes.

Key words visible light, organic photochemical reactions, electron donor-acceptor complex, photoexcitation, free radicals

1 Introduction

The utilization of visible light, the major component of sunlight, to induce significant chemical transformations is a sustainable and promising strategy in modern organic synthesis.[1,2] However, because most organic molecules cannot harvest photons in the visible light region, external photocatalysts such as transition metal complexes,[3] organic dyes,[4] or inorganic semiconductors[5] are usually required to enable single electron transfer (SET) or energy transfer (ET) (Figure 1). Since 2008, the research area of visible-light-induced organic photochemical synthesis has regained attention from the synthetic community and flourished in different aspects due to the remarkable work of the MacMillan, Yoon, and Stephenson groups.[6] In 2013 and 2016, two elegant reviews by MacMillan and co-workers extensively summarized the recent advances in visible light photoredox catalysis in organic synthesis with transition metal complexes as photocatalysts.[3] In 2014 and 2016, Nicewicz and co-workers produced two summaries of the use of organic dyes as photocatalysts in synthetic transformations.[4] In 2014, Lang, Chen, and Zhao prepared a comprehensive review to highlight organic transformations with heterogeneous visible light photocatalysts.[5]

In contrast to this mainstream scenario, several cases exist in which organic transformations are driven by visible light without external photocatalysts. The recent surge in this field shows that synthetic chemists have taken serious notice and started to realize the great potential of this strategy. For example, in 2013, the Melchiorre group found that an electron donor-acceptor (EDA) complex between key chiral enamine intermediates and substrates allowed visible-light-promoted organocatalytic asymmetric alkylations of aldehydes without requiring an external photosensitizer.[7] Later, a diverse variety of photocatalyst-free organic photochemical transformations were developed. Despite these impressive contributions, no review dedicated to this interesting topic has been produced. Therefore, in this review we will endeavor to summarize the recent advances in visible-light-driven, photocatalyst-free organic reactions according to the following photoexcitation modes: (1) visible light photoexcitation of a single substrate, (2) visible

Biographical Sketches

Yi Wei was born in 1991 in Hubei, P. R. China. She received her B.Sc. from Wuhan Textile University in 2013. After that, she started her Ph.D. studies under the supervision of Prof. Liang-Qiu Lu and Prof. Wen-Jing Xiao at Central China Normal University, working on asymmetric transition metal catalysis and organic photochemical synthesis.

Quan-Quan Zhou was born in the Jiangxi Province, P. R. China. In 2013, he obtained his B.Sc. at Jiangxi Normal University. He is currently carrying out his Ph.D. on visible-light-induced photochemical synthesis under the direction of Prof. Liang-Qiu Lu and Prof. Wen-Jing Xiao at the Central China Normal University

Fen Tan was born in 1986 in Hubei, P. R. China. She obtained her B.Sc. degree from Dezhou University in 2008 and received her Ph.D. degree in 2014 under the supervision of Prof. Wen-Jing Xiao at Central China Normal University. Currently, she is a lecturer at Hubei University of Education. Her research interests focus on green synthetic chemistry and asymmetric catalysis.

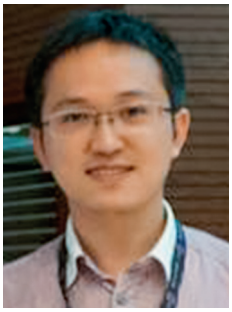

Liang-Qiu Lu was born in Zhejiang, P. R. China. He received his B.S. in Applied Chemistry in 2005 and obtained his Ph.D. degree in 2011 under the guidance of Professor Wen-Jing Xiao at Central China Normal University (CCNU). Then, he joined the College of Chemistry at CCNU as a Lecturer. From 2011 to 2013, Dr. Lu worked as a Humboldt postdoctoral fellow with Prof. Matthias Beller at the Leibniz-Institut für Katalyse e.V., Germany. In 2015, Dr. Lu became a full professor in the College of Chemistry at CCNU, China. His current research interests focus on transition-metal-catalyzed dipolar cycloadditions and visible-light-driven organic photochemical reactions.

Wen-Jing Xiao was born in 1965. He received his B.Sc. in chemistry from Central China Normal University (CCNU) in 1984 and then his M.Sc. under the supervision of Professor Wen-Fang Huang in 1990 at the same university. In 2000, he received his Ph.D. under the direction of Professor Howard Alper in University of Ottawa, Canada. Following postdoctoral studies with Professor David W. C. MacMillan (2001–2002) at Caltech, USA, in 2003, Dr. Xiao became a full professor in the College of Chemistry at CCNU, China. His current research interests include the development of new synthetic methodologies and the synthesis of biologically active compounds.

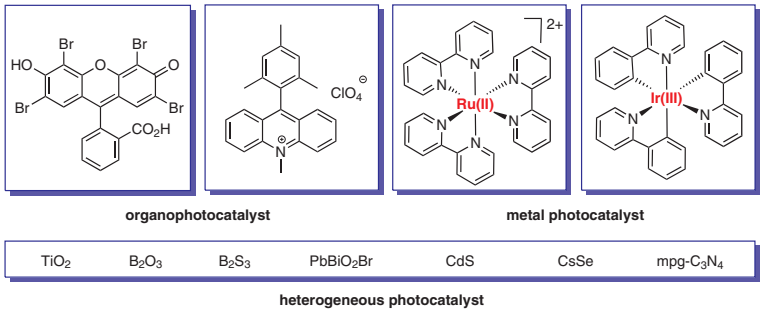

Figure 1 Representative photocatalysts used in organic synthesis

light photoexcitation of reaction intermediates, (3) visible light photoexcitation of EDA complexes between substrates, (4) visible light photoexcitation of EDA complexes between substrates and reaction intermediates, and (5) visible light photoexcitation of products.

2 Visible Light Photoexcitation of a Single Substrate

N-Bromoamides are a set of easily available and benchstable reagents that can deliver unique N-centered radicals through homolytic cleavage when irradiated by visible light, and these radicals can be further used for site-selective C–H functionalization. In 2007, Ramaswamy, Waghmode, and Arbuj reported the photochemical α-bromination of ketones **1** using NBS at room temperature without the use of an external catalyst (Scheme 1).[8] In addition to the cyclic ketones, a series of acyclic ketones were converted into the corresponding α-brominated products **2** in excellent yields within a few minutes. A blueshift of the absorption wavelength when adding the reaction mixture to the solution of 2,2-diphenyl-1-picrylhydrazyl (DPPH) in ethanol demonstrated that this process involved a radical pathway.

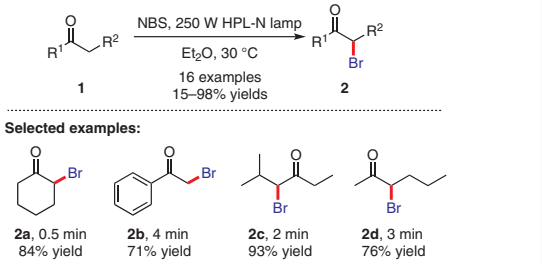

Scheme 1 Visible-light-promoted α-bromination of ketones

Based on this strategy, in 2014 Luo and co-workers developed a catalyst-free imidation of arenes **4** enabled by visible light photolysis of *N*-bromosaccharin (**3**) to produce the corresponding *N*-arylsulfonamides **5** with high efficiency (Scheme 2).[9] Moreover, this method was further applied to the synthesis of heteroarene imidation products **6** (39–90% yields). Pyridine, indole, and benzofuran were tolerated under the standard reaction conditions, furnishing the corresponding products **6a–c** in moderate to good yields.

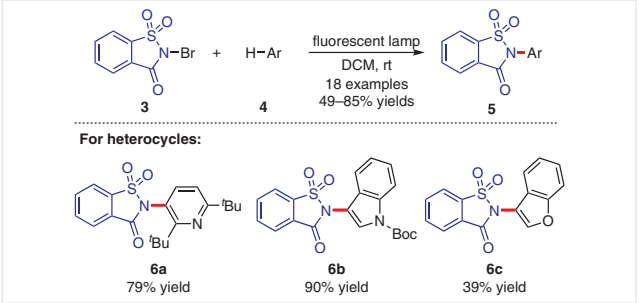

Scheme 2 Visible-light-driven and photocatalyst-free imidation of arenes and heteroarenes

A possible radical homolysis/substitution pathway is proposed for this process (Scheme 3). First, the controllable homolysis of *N*-bromosaccharin (**3**) is induced by visible light, generating saccharin N-radical **A** and a Br radical. Then, the key N-radical addition to arene **4** gives a cyclohexadienyl-type radical intermediate **Int-1**, which undergoes a further inner or outer sphere radical quenching to give **Int-2** and **Int-3**. The final consecutive electron/proton transfer processes of these two intermediates deliver the imidation product **5**. Based on the observed on-off photoresponsive behaviors in in situ monitored and control experiments, a radical propagation pathway was ruled out.

Also in 2014, the Alexanian group reported a site-selective bromination of unactivated aliphatic C–H bonds, such as in methylcyclohexane (**7**). This intermolecular functionalization was enabled by visible light irradiation in the absence of any photocatalyst and the readily available *N*-bromoamides **8** were used as a bromo source, giving the corresponding adducts **9** in useful chemical yields (Scheme 4).[10a] Notably, the high efficiency of this approach permitted the use of the substrate as the limiting reagent. Moreover, the functionalization of the *N*-phthalimide derivative of memantine **10** using *N*-bromoamide **8a** delivered the tertiary bromination product **11** in 70% isolated yield with complete

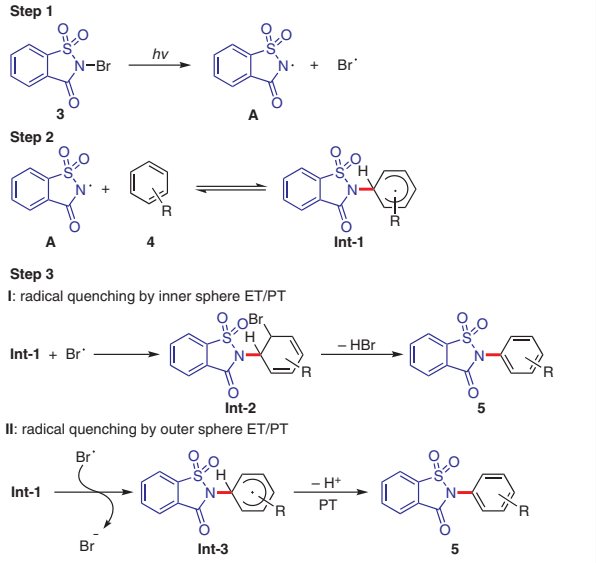

Scheme 3 Proposed mechanism for the visible-light-driven imidation of arenes and heteroarenes

regiocontrol. In addition, the terpenoid natural product (+)-sclareolide, with diverse electronic and steric control elements, was also investigated. Bromination of (+)-sclareolide (**12**) with *N*-bromoamide **8b** as the efficient N-radical precursor under visible light irradiation provided the C2-equatorial bromination product **13** as a single isomer.

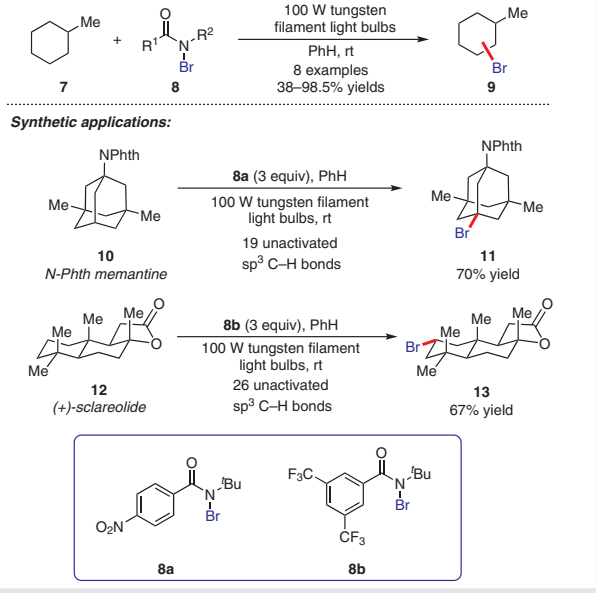

Scheme 4 Visible-light-promoted bromination of aliphatic C–H bonds

In 2016, the Alexanian group further extended this strategy to the regioselective chlorination of aliphatic C–H bonds such as in methylcyclohexane (**7**), using readily available *N*-chloroamide **14**, affording the corresponding adduct **15** with excellent chemo- and regioselectivity (Scheme 5).[10b] It is worth noting that the methodology could be applied to unsaturated substrates, which are challenging in the chemoselective functionalization of aliphatic C–H bonds. Unlike the previous work with site-selective bromination, one equivalent of base was necessary to act as a chloride scavenger, which significantly reduced the background reaction to improve regioselectivity. Importantly, this transformation was applied to the synthesis of (+)-chlorolissoclimide (**17**). Starting from commercially available (+)-sclareolide (**12**), chlorination product **16** was obtained in 82% yield; a subsequent eight-step sequence gave the final product **17** in 8–14% overall yield.

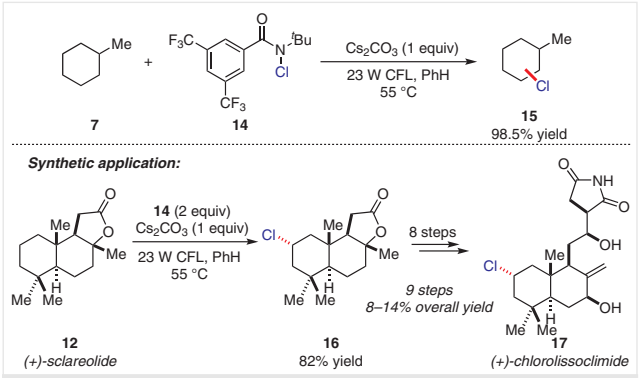

Scheme 5 Visible-light-driven chlorination of aliphatic C–H bonds

Photoactivation of bromoalkynes can also trigger C–Br bond homolytic cleavage to deliver alkynyl radicals. In 2018, an oxidative amidation of bromoalkynes **18** with anilines **19** under an O_2 atmosphere with irradiation by visible light was reported by Wang, Meng, and co-workers (Scheme 6).[11] The reaction was performed without an external photocatalyst under mild conditions, and a variety of α-ketoamides **20** were afforded in good yields. Additionally, based on control experiments, the oxygen in the products was believed to come from O_2 and not from H_2O.

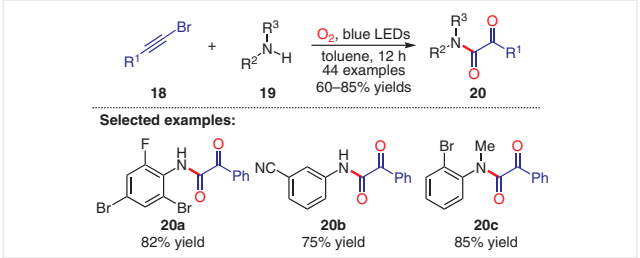

Scheme 6 Visible-light-promoted oxidative amidation of bromoalkynes

Dinitrophenylsulfonyloxy (ODNs) is a type of subunit that can be chemoselectively triggered by visible light to generate N-radicals. In 2013, the MacMillan group reported an asymmetric α-amination of aldehydes **21** by combining

visible light photoredox catalysis with asymmetric amine catalysis. N-radicals were formed using ODNs as a traceless activation handle via visible light photoexcitation, which then underwent enantioselective α-addition to chiral enamines to achieve stable α-aminoaldehydes **24** in moderate to good yields with high enantioselectivity (Scheme 7).[12] Amine catalyst **23** was identified as the best chiral catalyst for this transformation.

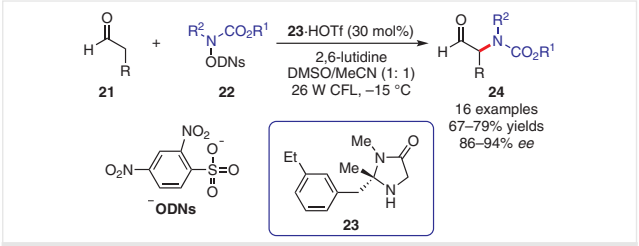

Scheme 7 Enantioselective α-amination of aldehydes catalyzed by the combination of photoredox catalysis and amine catalysis

A plausible mechanism is shown in Scheme 8. By exposing **22** to visible light, the photoexcitation of amine reagent **22** delivers the excited state **22***, which undergoes a single electron reduction and mesolysis of the N–O bond to generate N-radical **B** and the ODNs anion. Then, an asymmetric addition of N-radical **B** to chiral enamine **A**, derived from amine catalyst **23′** and aldehydes **21**, produces alkyl radical intermediate **C**. A single electron transfer from the alkyl radical to the photoexcited state **22*** furnishes iminium ion **D** with the release of the N-radical to the next round of the catalytic cycle. Hydrolysis of **D** delivers the enantioenriched α-aminoaldehydes **24** and regenerates the organocatalyst **23′**.

In 2014, the Maruoka group reported a mild method for generating acyl radicals from a series of branched aldehydes to give the hydroacylated products **28** with good efficiencies (Scheme 9).[13] In this case, the catalytic amount of hypervalent iodine reagent **27** undergoes a homolytic cleavage upon irradiation with visible light, thus acting as a radical initiator in the process. The reaction accommodated a variety of branched aldehydes **25** and substituted alkenes **26** with distinct geometries, producing the corresponding adducts **28** in moderate to good yields. In this selective hydroacylation approach, the hypervalent iodine catalyst **25** does not require high energy input, such as UV light, to enable homolysis, and this enables the superb selectivity of hydroacylation of branched aldehydes, given the facile decarbonylation of acyl radicals from various branched aldehydes.

In 2015, a photocatalyst-free protocol for the transformation of α-bromo ketones **29** through efficient radical generation under visible light irradiation was reported by You, Cho, and co-workers (Scheme 10).[14] This synthetic

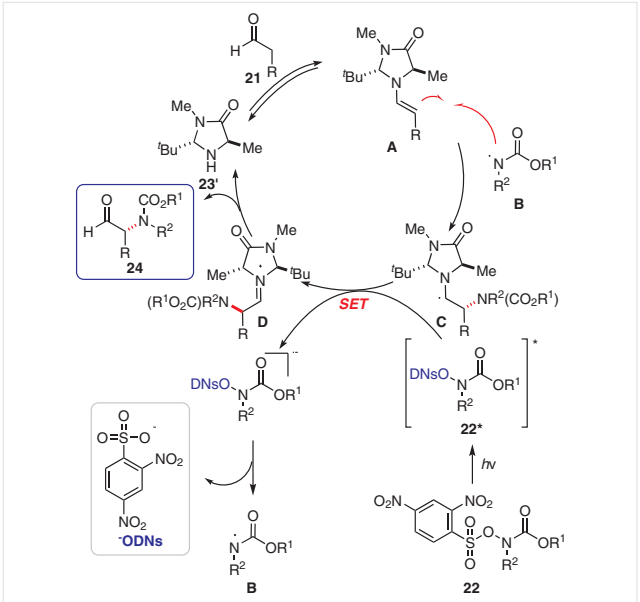

Scheme 8 Possible mechanism for aldehyde α-amination

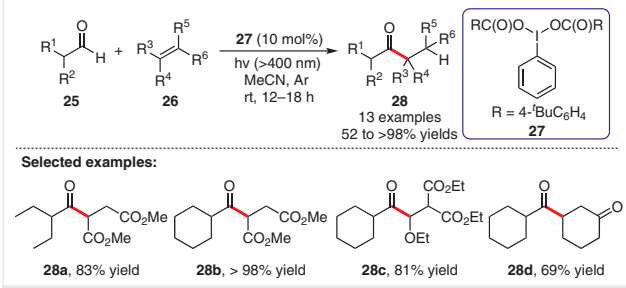

Scheme 9 Selective hydroacylation of branched aldehydes with electrophilic alkenes

process exhibited good functional group tolerance under environmentally benign conditions. In this process, the photoexcitation of Hantzsch ester (HE) induces single electron transfer within an encounter complex. The generated radical species can further react with oxygen and Hantzsch ester, delivering reductive debromination and α-hydroxylation products **30** and **31**, respectively.

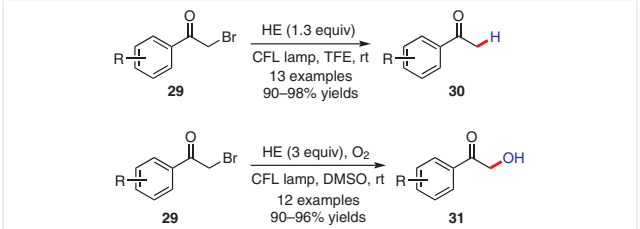

Scheme 10 Debrominative reduction and hydroxylation of α-bromo ketones

Elegant experiments revealed that Hantzsch ester could be photoactivated to initiate reactions via an energy transfer process. Li, Cheng, and co-workers disclosed an efficient method for converting vicinal dibromo compounds **32** into alkenes **34** (Scheme 11).[15] In the presence of Na_2CO_3, Hantzsch ester **33** acts as a self-activating reductant under visible light irradiation. The strategy features satisfactory substrate generality and functional group compatibility.

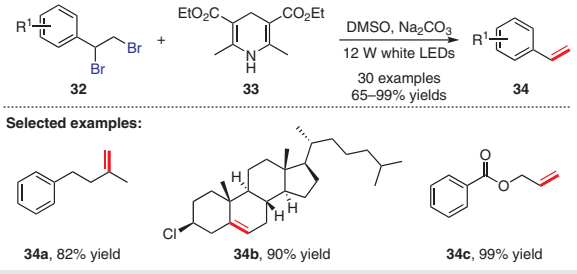

Scheme 11 Visible-light-driven debromination reactions of vicinal dibromo compounds

In 2017, the Melchiorre group found that 4-alkyl-1,4-dihydropyridines (alkyl-DHPs) can approach their electronically excited states by being exposed to violet light, thus triggering the formation of C(sp^3)-centered radicals without any external photocatalysts. This photochemistry successfully enabled a nickel-catalyzed C(sp^2)–C(sp^3) cross-coupling of aryl bromides **35** or acyl chlorides **36** with 4-alkyl-1,4-dihydropyridines **37**, which delivered the benzylated products **38** or ketones **39**, respectively, in good yields (Scheme 12).[16a]

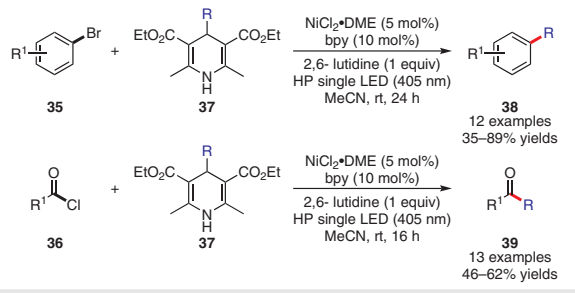

Scheme 12 Photoexcitation of alkyl-DHPs for cross coupling with aryl bromides or acyl chlorides

A possible reaction mechanism is proposed for this coupling reaction. As depicted in Scheme 13, the key to the success was attributed to the dual reactivity profile of the excited states of alkyl-DHPs **37***. First, they can act as strong reducing agents to regenerate Ni^0 catalyst **C** from Ni^I–X intermediate **F**. Second, they can also efficiently provide alkyl radicals after the single electron oxidation and homolytic cleavage processes. On the basis of these two points, the photochemical process and organometallic catalysis inter-

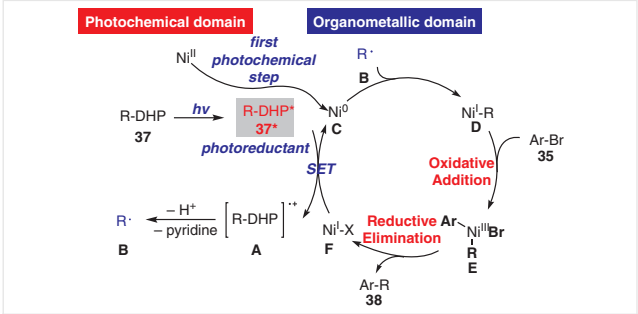

Scheme 13 Proposed mechanism for the cross coupling of aryl bromides or acyl chlorides with alkyl-DHPs

weave with each other, finally producing the desired coupling products under mild conditions.

In 2019, the Melchiorre group also discovered that easily accessible 4-acyl-1,4-dihydropyridines **41** can release acyl radicals under visible light irradiation. Based on this information, they realized an asymmetric conjugate addition of enals **40** with acyl radicals via an iminium catalysis mechanism in the presence of chiral secondary amine **42** and visible light, leading to optically active 1,4-dicarbonyl products **43** (Scheme 14).[16b]

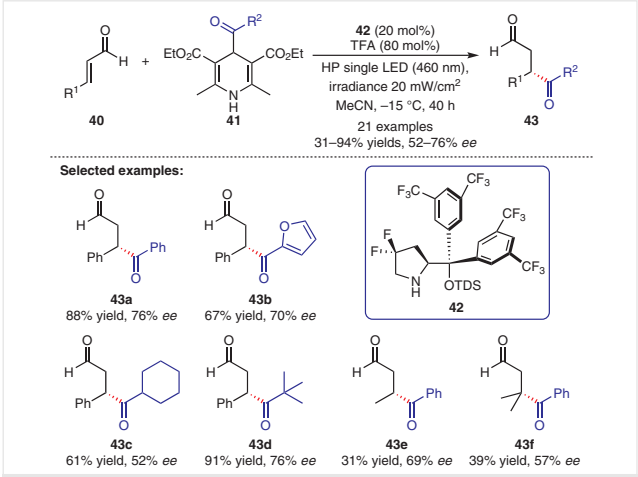

Scheme 14 Photochemical organocatalytic acyl radical addition to enals

In 2016, the Xu group reported a visible-light-induced and photocatalyst-free decarboxylative amidation reaction of α-keto acids **44** with amines **45** (Scheme 15).[17a] Mild conditions, simple operation, and satisfactory functional group tolerance made this methodology an attractive protocol for the construction of amides **46**. Control experiments proved that visible light and oxygen were necessary for this transformation. Trapping singlet oxygen with various scavengers demonstrated that photoexcited singlet oxygen existed in the system. Though no more information was provided by

the authors, it was possible that α-keto acids act as a photosensitizer in this reaction according the fact that carbonyl can function as photosensitizer.[17b,c]

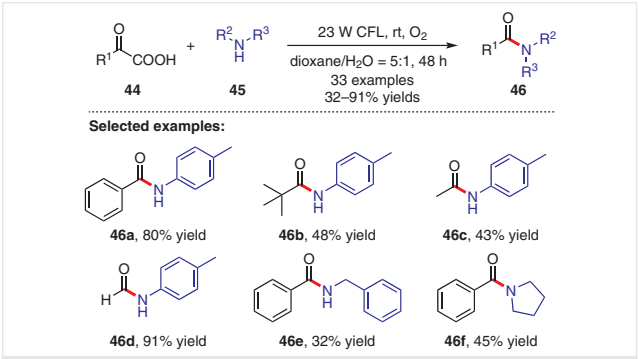

Scheme 15 Oxygen-promoted decarboxylative amidation

The proposed mechanism is depicted in Scheme 16. Condensation between α-keto acids **44** and amines **45** first leads to α-imino acids **47**. Then, $^1O_2$, generated from oxygen under the irradiation of visible light, abstracts a hydrogen from the α-imino acid to form radical **A**, which then undergoes decarboxylation to generate *N*-arylimidoyl radical **B**. Subsequent radical coupling gives enol compounds **48**, which then afford amides **46** through a tautomerization process. Notably, an $H_2{}^{18}O$ labeling experiment was performed to support the hydrolysis of the *N*-arylimidoyl radical by water, in which the ^{18}O isotope was detected in the amide products.

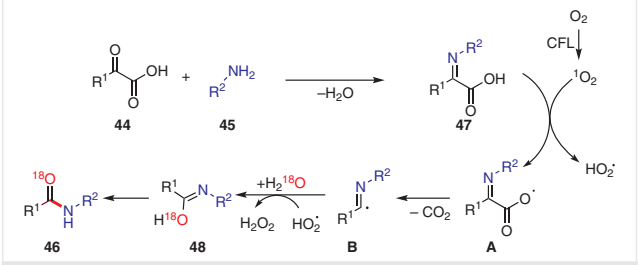

Scheme 16 Proposed mechanism for oxygen-promoted decarboxylative amidation

Also in 2016, the visible-light-promoted oxidative coupling reaction of phenols **49** and cyclic anilines **50** was reported by the Xia group using $K_2S_2O_8$ as an oxidant (Scheme 17).[18] A possible mechanism is depicted as follows: under visible light irradiation, the sulfate radical anion is formed as a strong oxidant to generate the radical intermediates **B** and **D**, respectively. Then, the radical cross-coupling reaction occurs to generate intermediate **E**, which isomerizes to give the final product **51**.

Quinolin-2-ones are a class of important aza-heterocycles with many biological activities, such as antibiotic and anticancer activity. Chu and co-workers reported a decarboxylative coupling/intramolecular cyclization cascade between tetrahydroquinolines **52** and 2-aryl-2-oxoacetic acids **53** induced by visible light (Scheme 18).[19] The one-pot procedure represents a mild and efficient way to approach various 4-arylquinolin-2-ones **54**. It is noteworthy that the current protocol can be utilized for the synthesis of an HBV inhibitor.

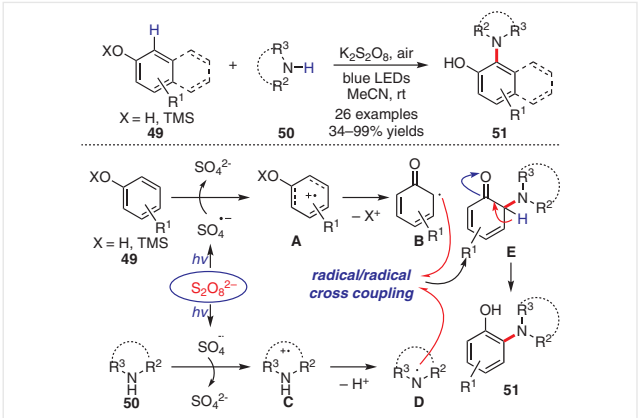

Scheme 17 Visible-light-promoted direct amination of phenols

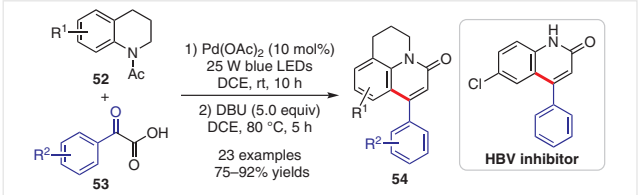

Scheme 18 Visible-light-driven decarboxylative coupling–intramolecular cyclization cascade

A rational mechanistic illustration for this transformation is depicted in Scheme 19. 2-Oxo-2-phenylacetic acid (**53a**) absorbs visible light to generate the benzoyl radical **B** through a decarboxylation process. Then, addition of radical **B** to the intermediate **A**, generated from substrate **52a** via Pd-catalyzed C–H activation, results in intermediate **C**. After that, reductive elimination together with the subsequent aldol condensation and DBU-promoted dehydration proceed to deliver the final product **54a**.

In 2017, Lu, Xiao, and co-workers detailed a novel asymmetric [4+2] cycloaddition of 4-vinyl-3,1-benzoxazinan-2-ones **56** with an array of ketene intermediates through a visible light photoactivation and palladium catalysis sequence. This process enables the effective construction of chiral quinolinones **59** containing all carbon quaternary stereocenters (Scheme 20).[20a] In this process, the ketenes were generated transiently in situ via photoinduced Wolff rearrangement of diazo ketones **57** by visible light irradiation. Notably, a chiral hybrid P,S ligand that they had developed in 2016 was the key for the high reactivity and stereo-

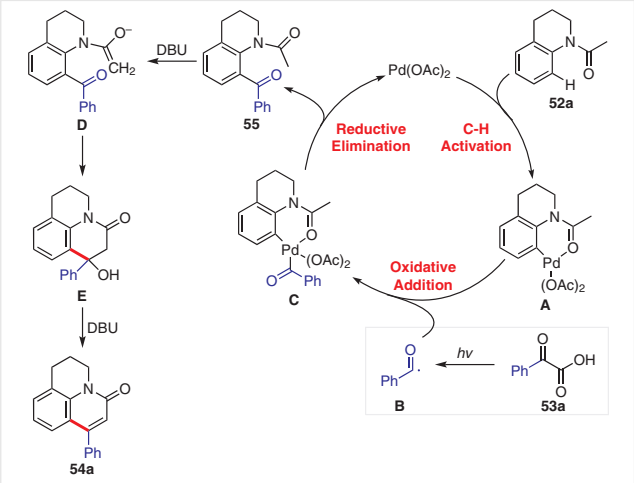

Scheme 19 Postulated mechanism for the visible-light-driven decarboxylative coupling–intramolecular cyclization cascade

control.[20b] This approach avoids the use of prepared ketenes, which are unstable under thermal conditions and poorly compatible with many transition metal catalysts. Importantly, the photochemical reactions show great advantages over thermal reactions involving prepared ketenes for generally higher efficiency and a broader substrate scope.

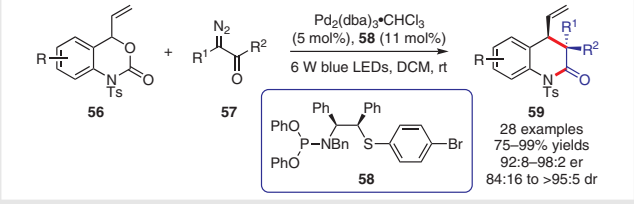

Scheme 20 Visible-light-photoactivated and palladium-catalysed cycloaddition

Based on a series of mechanistic investigations, a possible reaction pathway is proposed (Scheme 21). Initially, the visible light photoactivation of diazo ketone **57** promotes Wolff rearrangement to furnish the ketene intermediate **60** in situ. At the same time, the Pd-containing 1,4-dipolar intermediate **C** is formed after an oxidative addition/decarboxylation process. Subsequently, intermolecular nucleophilic addition and intramolecular Pd-catalyzed asymmetric alkyl allylation (AAA) occur to afford the desired chiral quinolinone **59** and finish the catalytic cycle. In 2018/2019, a similar photoactivation/metal- or organocatalysis strategy was applied to Pd-catalyzed enantioselective [5+2] cycloadditions,[20c] [3+2] cycloadditions,[20d] and divergent C- or O-acylation reactions of β-keto esters[20e] by using α-diazo ketones and visible light.

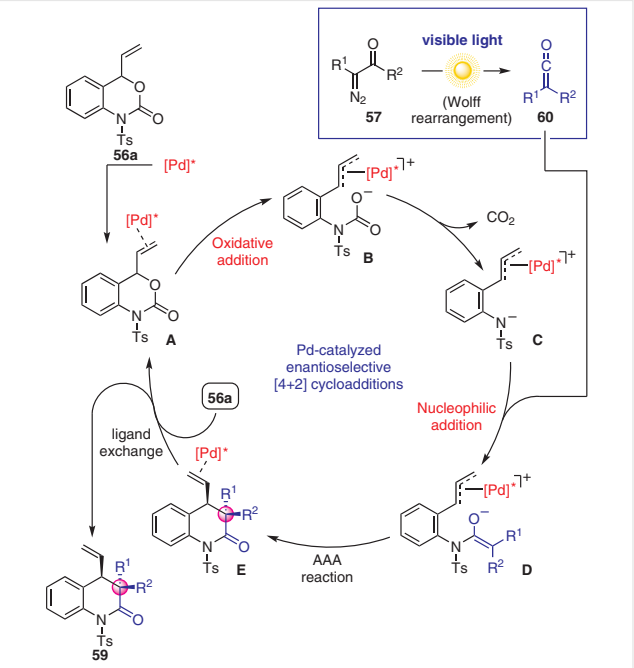

Scheme 21 Proposed mechanism for the visible-light-photoactivated and palladium catalysis cycloaddition

Siloxycarbenes are transient and nucleophilic acyl anion equivalents that can be easily generated from the photoexcitation of acylsilanes. The formation of these species is useful for carbene-mediated synthetic reactions, but they are less commonly applied in intermolecular C–C bond formation reactions. In 2018, the Kusama group described a photoinduced cross benzoin-type reaction between acyclic acylsilanes **61** and aldehydes **62** with the assistance of ZnI_2. This reaction provided a convenient access to synthetically useful α-siloxy ketones **63** (Scheme 22).[21]

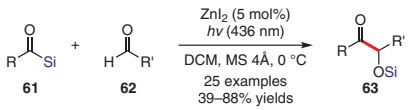

Scheme 22 Lewis acid catalyzed and visible-light-driven intermolecular coupling of acylsilanes and aldehydes

A plausible reaction mechanism including a role for ZnI_2 is shown in Scheme 23. Siloxycarbenes **A** are photochemically generated through the isomerization of acylsilanes **61**. Subsequently, **A** undergoes a nucleophilic addition to aldehyde **62**, which is electrophilically activated through coordinating to ZnI_2. Then, 1,4-silyl migration of a zwitterionic intermediate **B** affords the final product **63** accompanied by the regeneration of ZnI_2.

Acylsilanes have unique photochemical properties, and they can be easily converted into siloxycarbenes through Brook rearrangements. Siloxycarbenes can further react with various electrophiles. In 2012, Bolm and co-workers

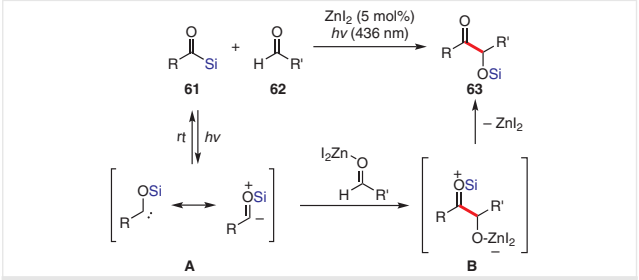

Scheme 23 Plausible mechanism for the intermolecular coupling of acylsilanes and aldehydes

developed photochemically induced silylacylations of alkynes **64**, which enabled a facile and effective synthesis of silylated chromanone derivatives **65** (Scheme 24).[22a] Aryl substituents on the alkynyl chain and acyl moiety were compatible with this reaction, furnishing the corresponding chromanones with good results. Moreover, substrates bearing either aliphatic groups or double bonds connected to the alkynyl moiety also proceeded smoothly under standard conditions, albeit with lower yields. However, no chromanone was obtained from an acylsilane containing a terminal triple bond.

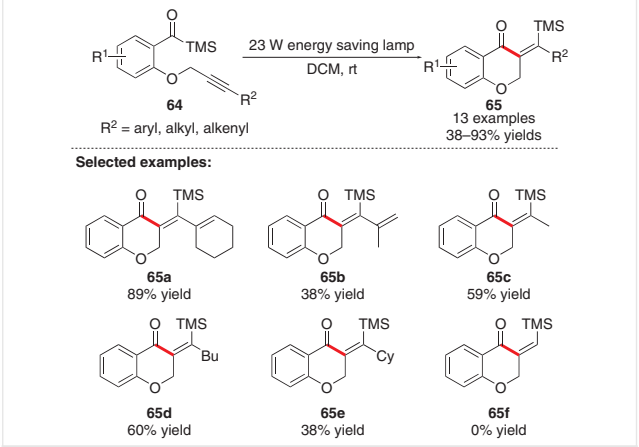

Scheme 24 Photoinduced silylacylations of alkynes

In 2014, they further applied this strategy to an intermolecular version and demonstrated that the presence of electron-deficient substituents on alkynes **67** are necessary for this transformation (Scheme 25).[22b] Various aromatic substituents on the acylsilane **66** were satisfactorily tolerated, providing a broad array of functionalized 2-aroylvinylsilanes **68** in high efficiency. Replacement of the aromatic substituents with heteroarenes, such as thiophene and furan, also gave the desired products in moderate yields.

The Minisci alkylation is of significance for the functionalization of arenes, particularly for electron-deficient arenes. In 2017, C.-J. Li and co-workers presented a trifluoromethylation of arenes **69** with trifluoro reagent **70** with-

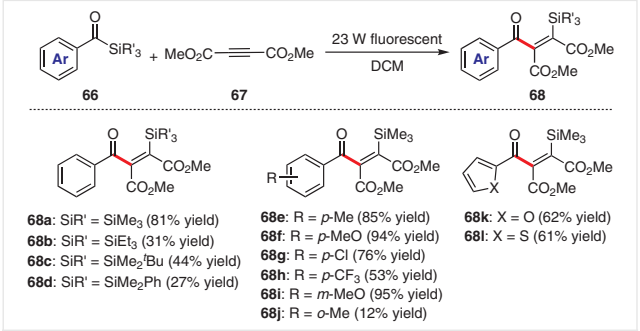

Scheme 25 Photoinduced intermolecular silylacylations of alkynes

out a photocatalyst (Scheme 26).[23] This transformation tolerates various functional groups and produces the corresponding products **71** in moderate yields.

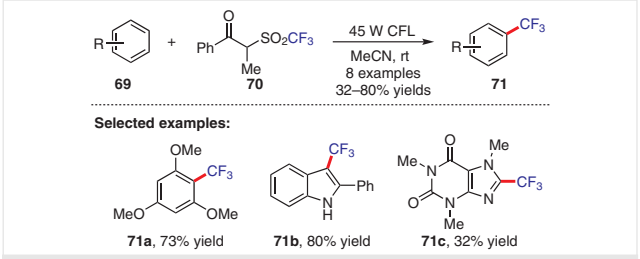

Scheme 26 Redox-neutral trifluoromethylation of arenes

From their continuous study of visible-light-photoredox catalysis, also in 2017 P.-H. Li, Wang, and co-workers found that the strategy also provided simple and efficient access to 3-sulfanyl- and 3-selanylindoles **74** via tandem cyclization between 2-alkynylanilines **72** and diaryl disulfides or diaryl diselenides **73** without a photocatalyst (Scheme 27).[24] Under the best reaction conditions, the protocol produced a wide range of diversely functionalized 3-sulfanyl- and 3-selanylindoles **74** in good to excellent yields. However, the protecting group of the 2-alkynylanilines was limited to tosyl and mesyl.

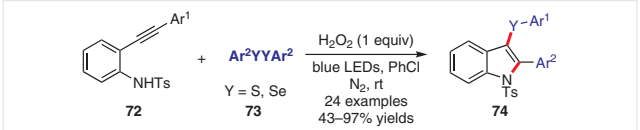

Scheme 27 Visible-light-induced tandem oxidative cyclization

Based on the preceding literature and radical capture experiments, a possible mechanism is proposed for this tandem reaction (Scheme 28). Under irradiation by blue LEDs, H_2O_2 underwent homolytic cleavage to produce hydroxyl radicals, which reacted with 2-alkynylaniline **72** through a single electron transfer (SET) pathway to form intermediate **A**. Intermediate **A** then undergoes an intramo-

lecular cyclization to furnish intermediate **B**. After a deprotonation process, intermediate **C** is afforded, which further interacts with diphenyl disulfide to give the desired product **74**.

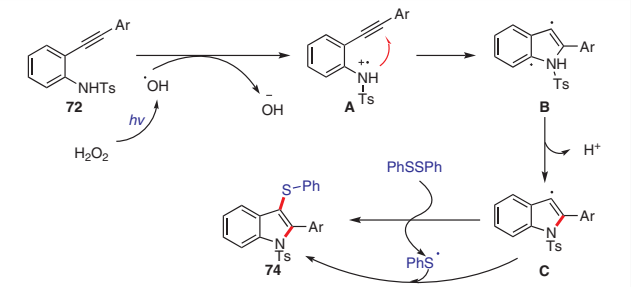

Scheme 28 Proposed catalytic cycle of tandem oxidative cyclization

The arylselenium radical could also be used in the construction of spiro compounds. In 2018, the Baidya group explored a visible-light-induced tandem radical cyclization/dearomatization reaction in the absence of photocatalyst, providing an efficient approach to selenium-substituted 1-azaspiro[4.5]decatrienediones **77** (Scheme 29).[25] Notably, they also reported a novel spiro-ring-opening strategy to construct densely functionalized acrylamides **78**, which can be demonstrated by the formation of ketimine **79** and its isomerization to aldimine **80**.

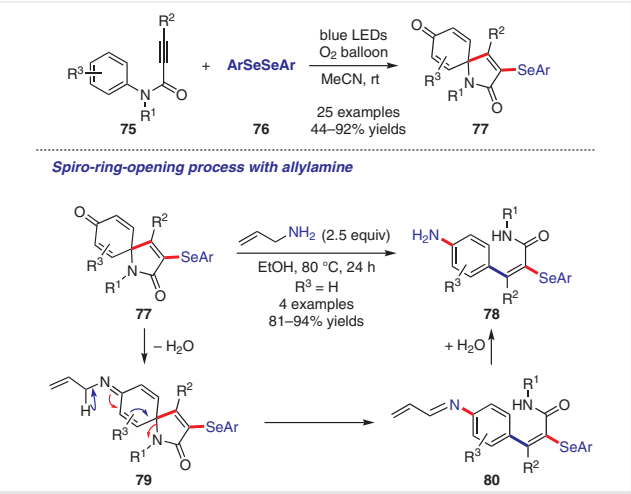

Scheme 29 Visible-light-induced selanylative spirocyclization and spiro-ring-opening process

As shown in Scheme 30, a tentative mechanism is proposed based on the results of control experiments. The arylselenium radical that is generated upon illumination with blue LEDs, adds to *N*-alkynoylanilines **75** to deliver radical **A**. A subsequent intermolecular radical *ipso*-cyclization occurs to afford radical intermediate **B**. In the oxygen atmosphere with diaryl diselenide, radical **B** is converted into intermediate **C**. Finally, the cleavage of the O–O bond leads to spirocyclized product **77**.

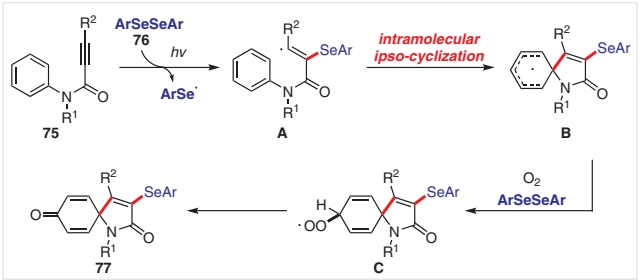

Scheme 30 Proposed catalytic cycle for the selanylative spirocyclization and spiro-ring-opening process

In 2018, the Studer group introduced a protocol for visible-light-promoted 1,2-carboboration of unactivated alkenes, in which bis(catecholato)diboron (**82**) serves as the boron source in association with alkyl halides **83** as the alkyl component (Scheme 31).[26a] The 1,2-carboboration products **84**, a class of synthetically valuable building blocks, were obtained in good yields. A visible-light-induced radical borylation of alkyl and aryl iodides was also successfully developed; DMF was the best solvent and played a vital role in this reaction.[26b]

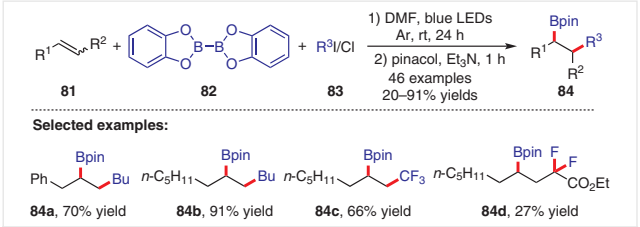

Scheme 31 Visible-light-mediated 1,2-carboboration of unactivated alkenes

A plausible mechanism is proposed to explain this transformation (Scheme 32). The key to the success of this reaction is the visible-light-mediated C–I bond homolysis of CF_3I to generate the trifluoromethyl radical. A cascade radical addition affords the radical **B**, which is then fragmented to boronic ester **E** and the reactive boryl radical **C**. Alternatively, adduct **B** decomposes and is trapped by DMF to give intermediate **D**. Cleavage of the B–B bond of this intermediate leads to the product **E** which can be converted into the final product **84** by treatment with pinacol and Et_3N.

The Studer group also developed an efficient methodology for the synthesis of functionalized allylboronic esters **88** via three-component coupling reaction (Scheme 33).[27] A set of allylboronates were produced from dienylboronates **85**, alkyllithium reagents **86**, and activated iodines **87** in generally moderate yields and high *trans* selectivity.

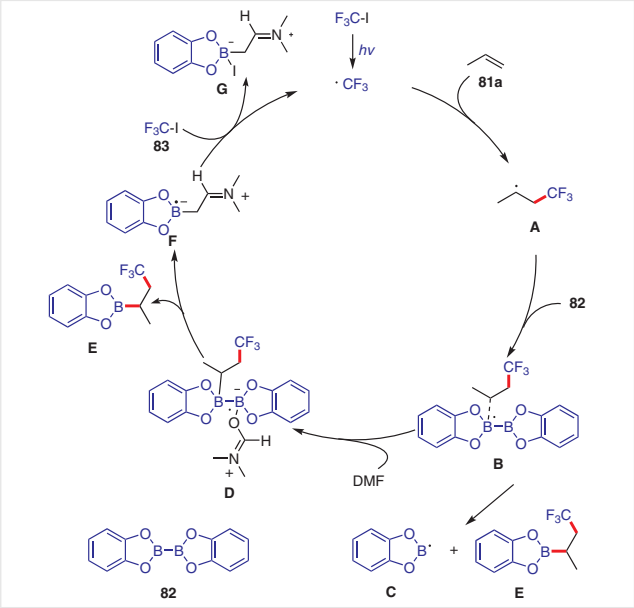

Scheme 32 Plausible mechanism for the 1,2-carboboration of unactivated alkenes

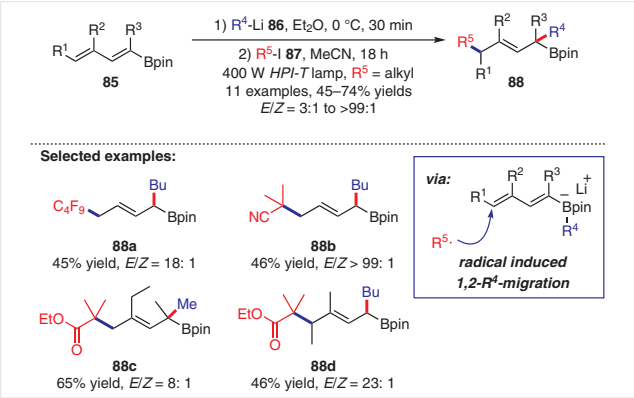

Scheme 33 Visible-light-initiated radical-polar crossover reactions

In 2017, a novel visible-light-promoted carboxylative cyclization of allylamines under CO_2 atmosphere was reported by the He group (Scheme 34).[28] A possible mechanism for the reaction is described in Scheme 35. Firstly, the n-$C_4F_9^{\bullet}$ radical was generated via a homolytic cleavage process under the irradiation of visible light. Then, addition of n-$C_4F_9^{\bullet}$ radical to carbamate intermediate **A**, which is formed from allylamines **89** and CO_2 in the presence of TBD (1,5,7-triazabicyclo[4.4.0]dec-5-ene), gives the carbon radical **B**. Then, the formation of intermediate **C** can occur via two different pathways and the following intramolecular cyclization affords the desired products **91**.

In 2017, Sarlah and co-workers reported the dearomative dihydroxylation of readily available arenes **92** with 4-methyl-1,2,4-triazoline-3,5-dione (**93**) as the arenophile,

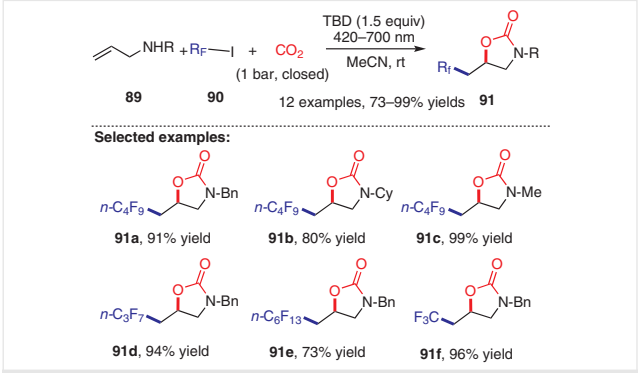

Scheme 34 Visible-light-induced carboxylative cyclization

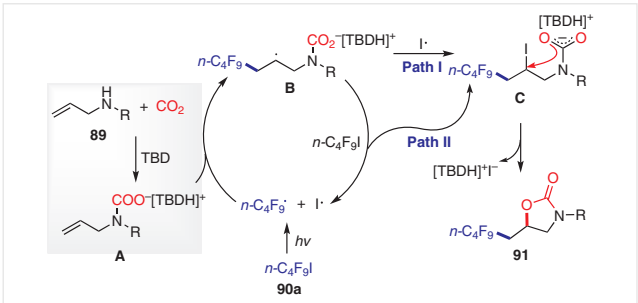

Scheme 35 Proposed mechanism for carboxylative cyclization

which affords an efficient approach to highly functionalized cyclohexenes **94** (Scheme 36).[29a] Upon irradiation by visible light, the arenophiles **93** are transformed into excited state **93*** that can form an exciplex with the ground state arene **92**. The generated exciplex then decomposes subsequently to form a cycloadduct **95**, which is further converted into diols **94** under dihydroxylation conditions. More importantly, the dearomative strategy was successfully applied to the construction of complex natural products, such as conduramine A and MK7607. Then, they further opened up a new avenue to explore the cycloadducts **95** through transi-

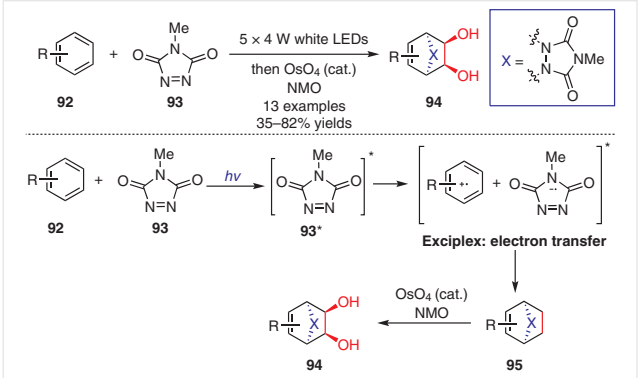

Scheme 36 Visible-light-induced dearomative dihydroxylations with arenophiles

tion metal catalysis. By using Pd or Ni as a catalyst, ring opening of the MTAD–arene cycloadduct with nucleophiles provided corresponding products in high efficiency and excellent selectivity.[29b–e]

3 Visible Light Photoexcitation of Reaction Intermediates

Olefin hydrogenation is among the most significant transformations in organic synthesis. Among various hydrogen sources, hydrazine is very cheap and abundant with high hydrogen content (12.5%). Moreover, hydrazine can be photoexcited by visible light to generate an active intermediate and initiate reactions. In 2014, Leow and co-workers reported a practical method for the photodriven diimide (diazene) reduction of alkenes **81**; this method produces the hydrogenated products **97** in generally good yields with N_2 as the only byproduct (Scheme 37).[30] In this process, the *cis* isomer of diimide is the reactive species. After oxidation of hydrazine **96** by oxygen from air, diimide is generated as an equal mixture of both *trans*-**A** and *cis*-**B** isomers. Isomerization from *trans* to *cis* is accelerated by irradiation from a compact fluorescent lightbulb (CFL). Then, reduction of the olefin **81** proceeds with *cis*-diimide through a six-membered transition state **C** to give the final product **97**.

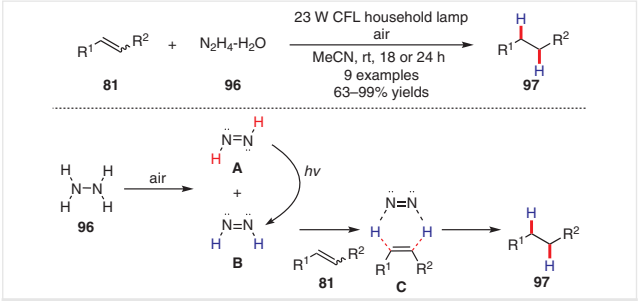

Scheme 37 Photoexcited reduction of alkenes with diimide

The benzimidazole structural motif has a broad range of biological functions. In 2014, Cho and co-workers reported an efficient approach for the construction of benzimidazoles **100** from *o*-phenylenediamine (**98**) and a variety of aldehydes **99** with oxygen as the oxidant (Scheme 38).[31] This methodology tolerated differently substituted arylaldehydes and alkylaldehydes, providing a new option for the synthesis of benzimidazoles.

Mechanistic studies demonstrated that a mixture of **98** and **99** resulted in a bathchromic shift in UV/visible absorption experiments, which indicated that an active intermediate was formed with visible light irradiation. A plausible mechanism is proposed for this process based on different experiments (Scheme 39). Condensation of diamine **98** with aldehyde **99** forms imine **A**, which is converted into its

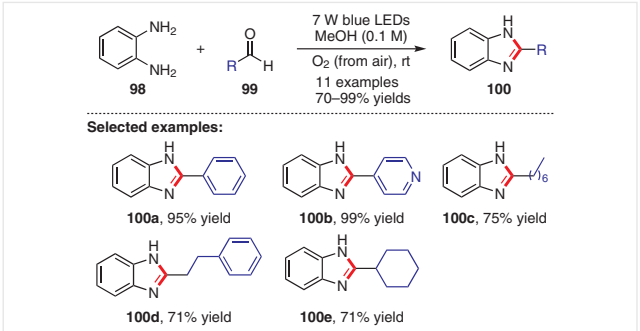

Scheme 38 Visible-light-promoted synthesis of benzimidazoles

excited state **A*** under visible light irradiation. The active intermediate transfers an electron to oxygen, forming a superoxide and a radical cation **B**, and then intramolecular radical cyclization and deprotonation produce intermediate **C**. Finally, hydrogen abstraction by the hydroperoxyl radical produces the desired benzimidazole **100** with the release of H_2O_2, which was detected by a H_2O_2 indicator.

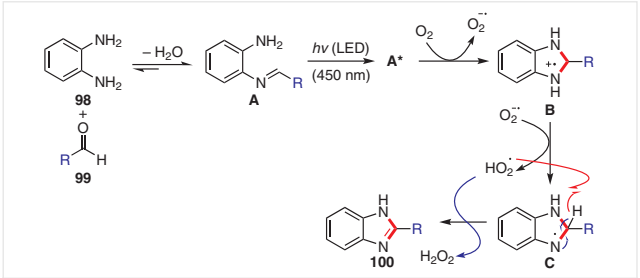

Scheme 39 Proposed catalytic cycle for the synthesis of benzimidazoles

In 2015, the Wang group reported a decarboxylative alkynylation of keto acids **44** with sunlight irradiation, utilizing hypervalent iodine reagent BI-OH **102** as photolysis catalysts in the absence of external photocatalyst and producing ynones **103** in generally good yields (Scheme 40).[32a] Moreover, the alkynyl bromide **101** could be accessed in situ from NBS, $AgNO_3$, and phenylacetylene. This methodology features simple operation and high functional group compatibility.

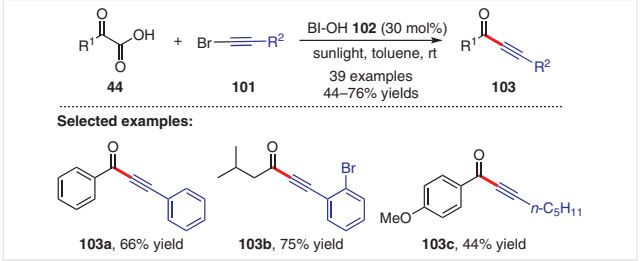

Scheme 40 Sunlight-promoted decarboxylative alkynylation of keto acids

Mechanistic studies involving reactions to determine possible intermediates and radical-trapping experiments using TEMPO and BHT indicated that this reaction might proceed via a free radical process with BI-alkyne as an important intermediate. As illustrated in Scheme 41, the reaction of BI-OH **102** with 2-oxo-2-phenylacetic acid (**44a**) formed compound **A**, which undergoes homolysis by irradiation with sunlight to generate iodanyl radical **B** and radical **D**. Then, radical **B** reacts with (bromoethynyl)benzene (**101a**) to furnish BI-alkyne intermediate **F** and a Br• radical. At the same time, the radical **D** transforms into benzoyl radical **E** with extrusion of CO_2, and radical addition to BI-alkyne generates intermediate **G**. Ynone **103a** is obtained from **G** with the release of radical **B**. Additionally, a radical coupling reaction between Br• radical and **B** produces **C**, and the subsequent hydrolysis regenerates BI-OH **102**.

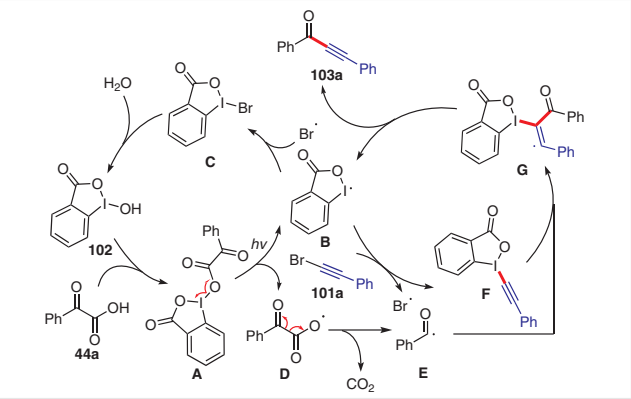

Scheme 41 Possible mechanism for the decarboxylative alkynylation of keto acids

Subsequently, the Wang group extended this strategy to the synthesis of functionalized oxindole skeletons via a tandem decarboxylative radical addition/cyclization process with keto acids **44** and acrylamides **104** (Scheme 42).[32b] In the presence of hypervalent iodine(III) reagent BI-OAc **105**, the cascade reaction proceeded smoothly, delivering the corresponding products **106** in good yields at room temperature. In this reaction, the energy from blue LEDs (450–455 nm) was sufficient to break the O–I bond of the intermediate, initiating the reaction without any photocatalysts.

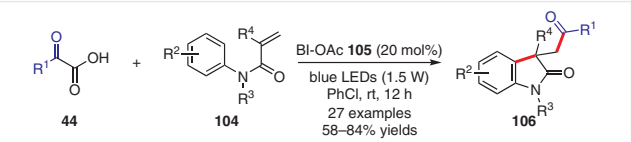

Scheme 42 Visible-light-driven decarboxylative acylarylation of acrylamides with keto acids

As depicted in Scheme 43, a plausible mechanism is proposed to illustrate this acylarylation reaction. First, the transesterification of BI-OAc **105** with 2-oxo-2-phenylacetic acid (**44a**) forms intermediate **A**. The homolytic cleavage of **A** under the illumination of blue LEDs generates benzoyl radical **B** and iodanyl radical **C** with the release of CO_2. This cleavage is considered the critical step in this cascade process. A free radical addition of benzoyl radical **B** to the C=C bond of acrylamide **104a** and the following intramolecular radical cyclization procedure form radical intermediate **D**. The abstraction of a hydrogen atom from **D** delivers the final product **106a**. Meanwhile, intermediate **E** is formed, which then reacts with **44a** to release H_2 and afford **A** that participates in the next cycle.

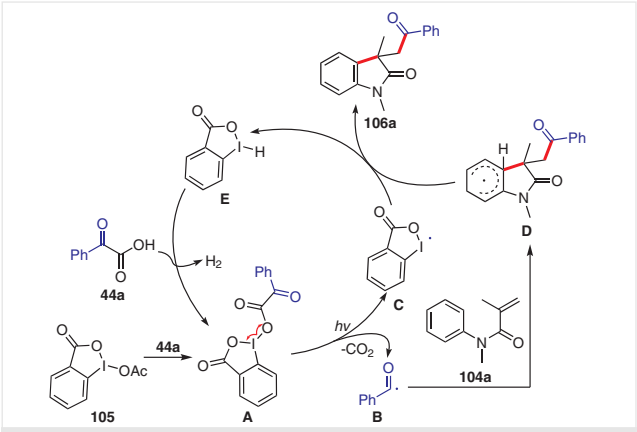

Scheme 43 Plausible mechanism for the decarboxylative acylarylation of acrylamides with keto acids

Many decarboxylative coupling reactions have been reported by using photoredox catalysis. In 2015, Overman and co-workers observed the visible-light-promoted coupling of *N*-(acyloxy)phthalimides with alkene acceptors in the absence of a photocatalyst, and this reaction required significant additional mechanistic investigation.[33a] In 2016, the Fu group developed an elegant method of visible light photoredox decarboxylative arylsulfanylation of *N*-(acetoxy)phthalimides **107** with arenethiols **108**, delivering the arylsulfanylation products **109** with high efficiency (Scheme 44).[33b] The mild catalytic system tolerated a variety of functional groups. Furthermore, the natural *cis*-octa-

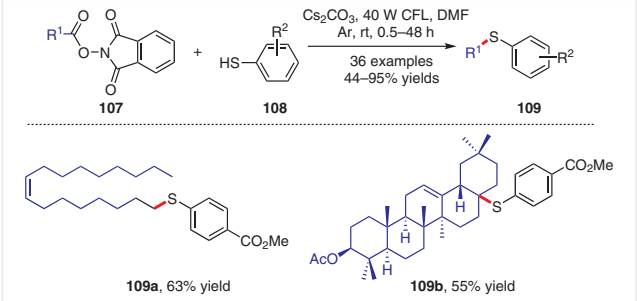

Scheme 44 Visible-light-induced decarboxylative arylsulfanylation of *N*-(acetoxy)phthalimides with arenethiols

dec-9-enoic acid and oleanic acid derivatives can be easily transformed into the corresponding arylsulfanylation products **109a** and **109b** smoothly, demonstrating the great potential of this method.

Based on the results of UV-visible absorption spectra, TEMPO trapping experiments, ^{15}N NMR spectroscopy, and Stern–Volmer fluorescence quenching experiments, a plausible catalytic reaction pathway is proposed (Scheme 45). Structures of **107** and **A** are resonant to each other. The intermediate **B** is provided by the complexation of **A** with Cs_2CO_3. Irradiation of **B** with visible light affords the excited state **B*** that undergoes a single electron transfer with the ArS anion to deliver intermediate **C** and an ArS˙ radical, the dimerization of which produces diaryl disulfide. Elimination of the phthalimide anion from **C** and the subsequent release of carbon dioxide provide radical **E**. Reaction of **E** with diaryl disulfide leads to the desired product **109**.

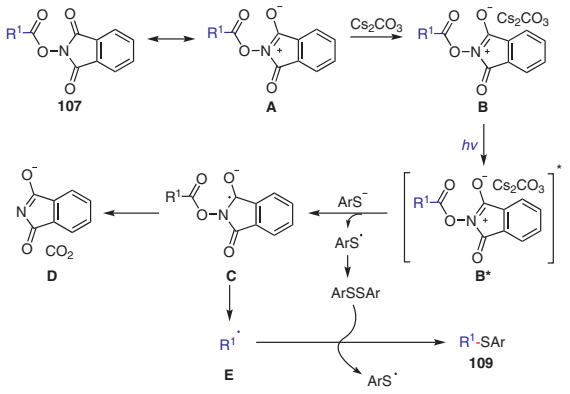

Scheme 45 Plausible reaction pathway for the decarboxylative arylsulfanylation of *N*-(acetoxy)phthalimides with arenethiols

The Fu group then reported visible-light-driven decarboxylative couplings of *N*-(acetoxy)phthalimides **110** with the assistance of thiophenol **111** as an efficient organocatalyst (Scheme 46).[33c] The corresponding intramolecular amination products **112** were obtained generally in good yields under visible light irradiation. Moreover, α,β-unsaturated ketones **113** and nitriles **114** were suitable for this process, delivering the decarboxylative addition products **115** and **116**, respectively, in good yields.

Another impressive example of decarboxylative functionalization was developed in 2017 by the Aggarwal group, who easily converted the widely available carboxylic acids **117** into versatile boronic esters **120**. Simply irradiating the *N*-hydroxyphthalimide ester derivatives of carboxylic acids **119** with visible light in the presence of bis(catecholato)diboron (B_2cat_2, **82**), a C–B bond is constructed in an efficient way under mild conditions (Scheme 47).[34a] In this reaction, dimethylacetamide (DMAc) played two roles: the best solvent and a boryl radical stabilizer. It is worth noting that

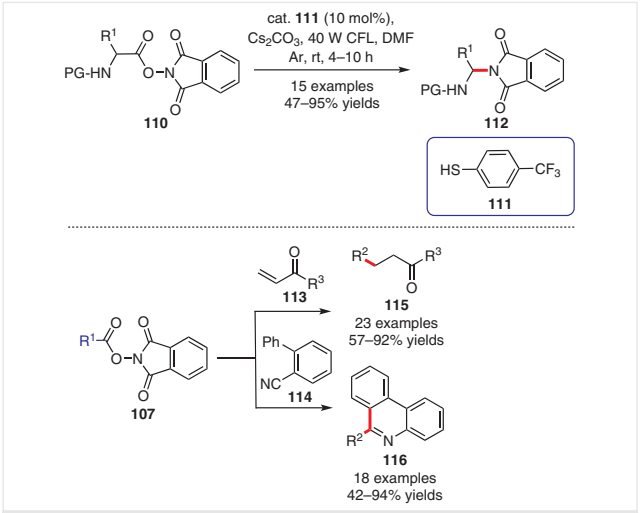

Scheme 46 Visible-light-driven decarboxylative couplings of *N*-(acetoxy)phthalimides

the transformation also generated the desired product in the dark albeit at a much lower rate, demonstrating that both a photochemical pathway and a less-efficient thermal pathway occur. Also in 2017, the Glorius group reported a decarboxylative borylation of *N*-hydroxyphthalimide esters through visible light photoactivation, which were produced in situ from the corresponding aryl carboxylic acids.[34b] Unlike the previous studies on decarboxylative functionalization, which are limited to alkyl carboxylic acids, this reaction can use aromatic *N*-hydroxyphthalimide esters as efficient aryl radical precursors.

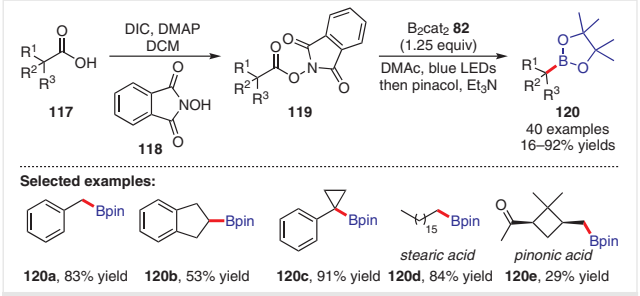

Scheme 47 Photo-promoted decarboxylative borylation of carboxylic acids

Based on the bathochromic shift phenomenon in the UV-visible absorption spectrum of *N*-hydroxyphthalimide and the boron reagent in DMAc solution, a proposed catalytic cycle is described (Scheme 48). Initially, substrate **119** and DMAc bind to the boron atom of B_2cat_2 **82**, forming intermediate **A**, which is stimulated with blue LEDs light and undergoes homolysis to form radicals **B** and **C**. Subsequently, decarboxylation of **C** forms intermediate **D** and the alkyl

radical **E**. The alkyl radical then reacts with intermediate **F**, generating the product **120** and DMAc-stabilized boryl radical **B**. This radical could either react with substrate **118** to give **G**, which undergoes homolytic decarboxylation to propagate the radical chain process, or the chain could be terminated through radical–radical dimerization. Alternatively, this reaction could be initiated by thermal homolytic fragmentation of the dimer.

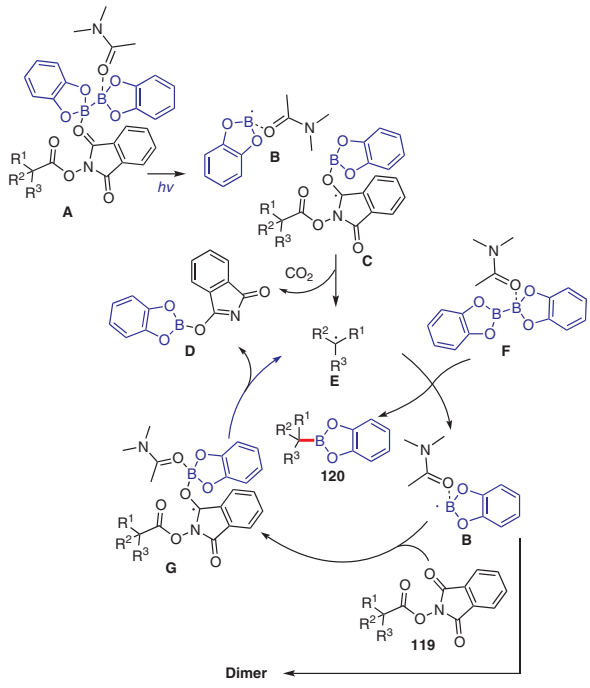

Scheme 48 Plausible mechanism for the decarboxylative borylation of carboxylic acids

Visible light irradiation of iodinated intermediates easily induces homolytic C–I cleavage, thus initiating radical reactions under relatively mild conditions. For instance, the Itoh group described an impressive intermolecular cyclopropanation of styrenes **122** with activated methylene reagents **121** in the presence of iodine and visible light irradiation. Styrenes with various substituents gave the corresponding cyclopropanes **123** with good results (Scheme 49).[35a] Importantly, equivalents of iodine and base were necessary to maintain the high efficiency of this reaction. Interestingly, changing the styrene to an alkene eliminated this reactivity.

A possible mechanism involving a chain reaction is also postulated for this tandem reaction (Scheme 50). Intermediate **A** is formed from the K_2CO_3-assisted iodination of activated methylene compounds **121**. The following photoinduced homolytic cleavage of intermediate **A** generates carbon radical **B**. Then, **B** attacks styrene **122** and produces

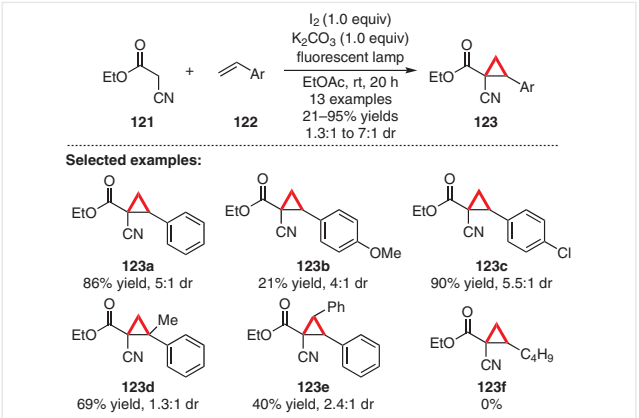

Scheme 49 Intermolecular cyclopropanation of styrenes

another intermediate **C**, which abstracts the iodine radical from **A** to afford intermediate **D**. Finally, 3-*exo*-tet cyclization of **D** occurs to deliver the desired cyclopropane **123**.

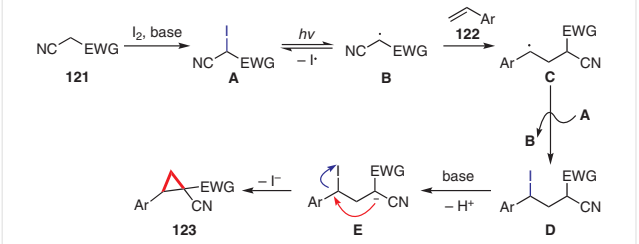

Scheme 50 Possible mechanism for the intermolecular cyclopropanation of styrenes

Han and co-workers also used this strategy for the production of spiro[2.4]heptane-4,7-dione derivatives **126** by NIS-initiated cascade spirocyclopropanation between 1,3-dicarbonyl compounds **124** and styrenes **125** (Scheme

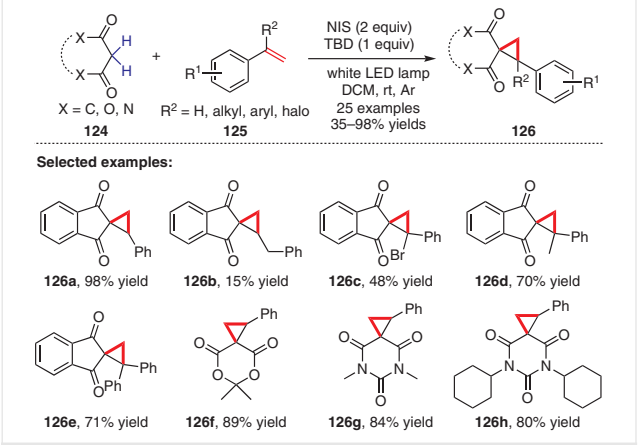

Scheme 51 NIS-initiated spirocyclopropanation of styrenes with 1,3-dicarbonyl compounds

51).[35b] The reaction could be conducted under simple conditions using white LEDs and tolerated a wide range of substrates, with good to excellent chemical yields.

The Itoh group achieved a photoinduced metal-free aerobic intramolecular cyclization of indole with malonates to produce ring-fused polycyclic heteroarenes **128** (Scheme 52).[36] For this reaction, the key intermediate with an iodinated malonate moiety was formed from the reaction of substrate and in situ generated I_2. Good to excellent yields of the corresponding products were obtained with the assistance of 20 mol% CaI_2 as the Lewis acid catalyst and oxygen as a green oxidant.

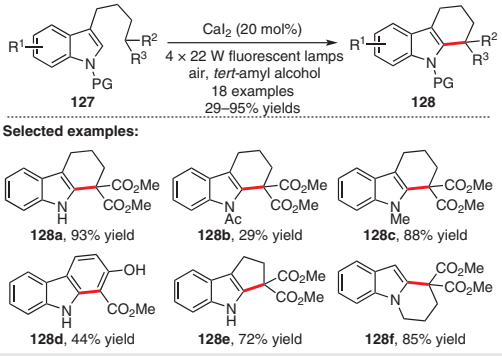

Scheme 52 Visible-light-driven, aerobic intramolecular dehydrogenative cyclizations of indoles

Mechanistic studies with the radical scavenger TEMPO suggested that this transformation proceeds through a free radical process. As illustrated in Scheme 53, initially, substrate **127a** reacts with I_2 generated in situ by the photooxidation of HI, thus affording the key intermediates **A** smoothly. Then, visible-light-driven homolytic cleavage of the C–I bond in intermediate **A**, and the following intramolecular cyclization and radical cross coupling with I• radical occur to give intermediate **C**. Finally, the desired product **128a** is generated after releasing HI. Notably, the reaction of intermediate **A** could also occur in the dark, which indicates that the reaction mechanism may also involve an ionic pathway.

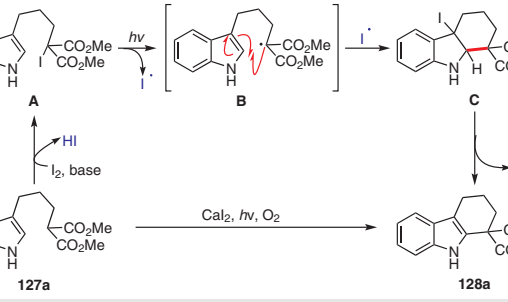

Scheme 53 Proposed photooxidative cyclization mechanism for the intramolecular dehydrogenative cyclizations of indoles

The Itoh group further applied the photooxidative cross dehydrogenative coupling strategy to obtain α-heteroarylated carbonyls **131** via the coupling of thiophenes **129** with carbonyls **130** (Scheme 54).[37] Control experiments indicated that I_2, visible light, and O_2 were necessary for this transformation. Substrates with various substituents such as amide, ketone, and sulfonyl groups were well tolerated under the standard conditions. However, diethyl methylmalonate and diethyl malonate were not suitable for this reaction.

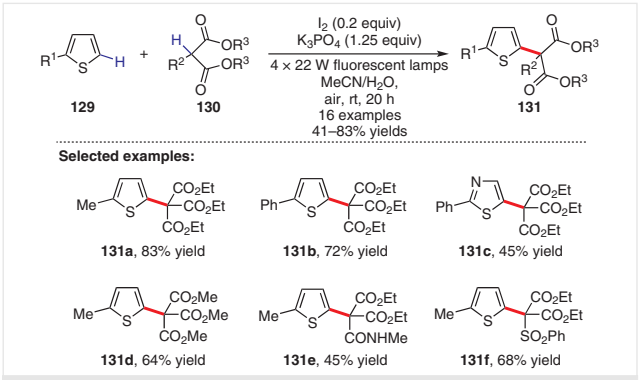

Scheme 54 Photoinduced cross dehydrogenative coupling

In 2015, Yuan and co-workers reported a direct C–H arylation of benzenes using 1,10-phenanthroline (**134**) as ligand. Under the standard conditions, a variety of aryl halides **132** with different functional groups were compatible in this reaction, affording the desired products **135** in high efficiency (Scheme 55).[38] A possible mechanism is illustrated. After irradiation by visible light, SET from KO^{t}Bu to 1,10-phenanthroline (**134**) in the interior of complex **A** provides

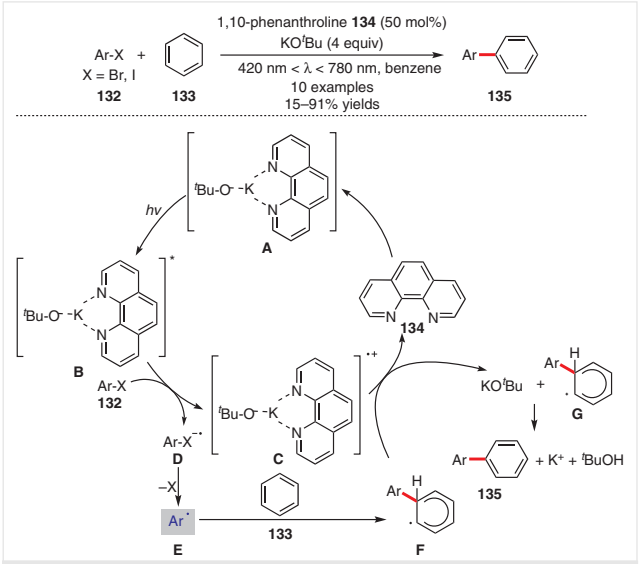

Scheme 55 Photoinduced biaryl synthesis and the possible mechanism

the phenanthroline radical anion. Then, the electron of the excited intermediate **B** is transferred to aryl halides **132** to give the aryl radical **E** and intermediate **C**. Radical addition of **E** and oxidation of **F** afford cation intermediate **G**, which will be transformed to the final products **135** with the assistance of KO^{t}Bu.

In 2017, Lu and Zhao reported that the monochlorination of cyclohexane (**136**) with Oxone as the oxidant under visible light irradiation selectively affords chlorocyclohexane (**137**) in high yield (Scheme 56).[39] This new chlorination of unactivated alkyl sp^3 C–H bonds was achieved by oxidation of chlorine anions with Oxone and successive generation of a Cl$^{\bullet}$ radical under irradiation.

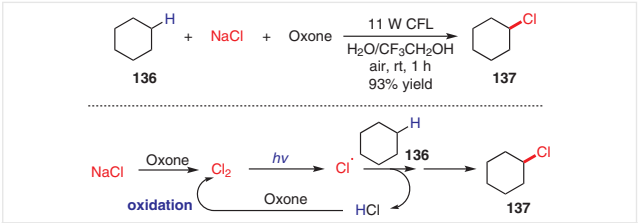

Scheme 56 Visible-light-induced oxidative chlorination of cyclohexane

In 2016, the Hashmi group described an impressive visible light photosensitizer-free intermolecular difunctionalization of alkynes **138** with arenediazonium salts **139** to afford a variety of α-aryl ketones **140** (Scheme 57).[40] In this transformation, the utilization of simple (4-$CF_3C_6H_4$)$_3$PAuCl and electron-deficient ligands dramatically increased the efficiency. This protocol features mild reaction conditions and shows good functional group compatibility.

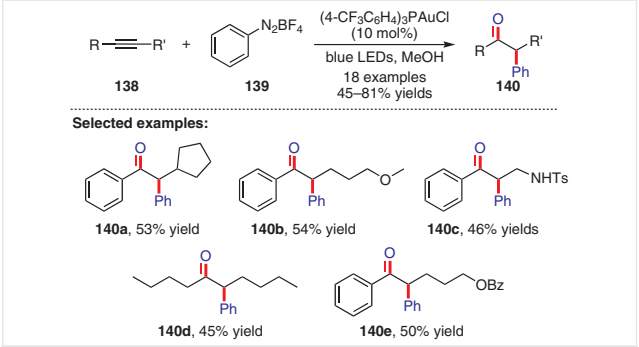

Scheme 57 Visible-light-mediated difunctionalization of alkynes

A highly speculative mechanism is proposed in Scheme 58 to explain this process. After a single electron transfer/radical recombination process, Au(III) species **B** is formed. This species is further sensitized by visible light to give Au(III) species **C** with the loss of nitrogen. Then, methanol addition to the Au-activated alkyne delivers vinyl gold

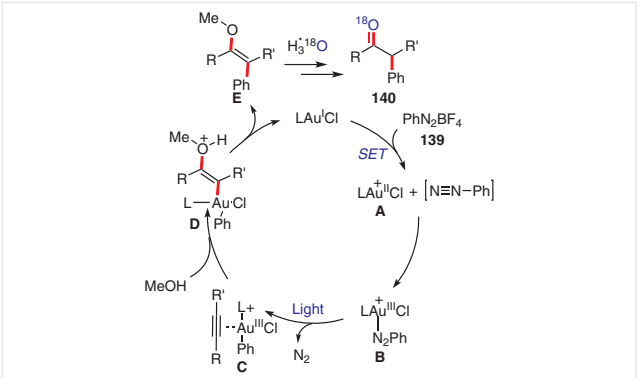

Scheme 58 Proposed mechanism for the difunctionalization of alkynes

species **D**. Reductive elimination and hydrolysis proceed to produce the final products **140**.

In 2017, the Hashmi group extended the success of visible-light-induced Au catalysis strategy to the C–C coupling reaction, thus providing an alternative route to various substituted biaryls **142** with satisfactory yields and broad functional group tolerance (Scheme 59).[41] It is worth noting that the boronic acids bearing electron-withdrawing groups on the benzene ring appeared to have more reactivity. This result illustrated that the boronic acids bearing electron-withdrawing groups can undergo a faster transmetalation.

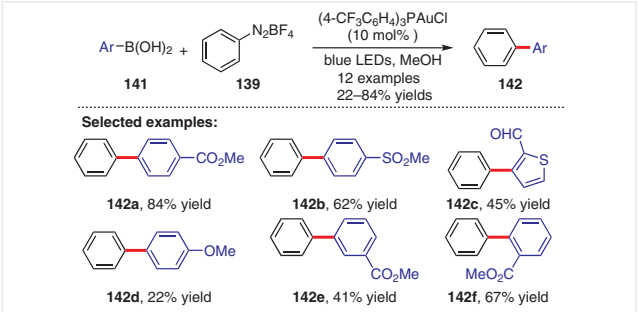

Scheme 59 Visible-light-induced Au catalysis for the C–C cross coupling

In 2018, Ackermann and co-workers increased the range of visible-light-induced C–H arylation of heteroarenes **143** with arenediazonium salts **139** to produce biaryls **144** in moderate to good yields (Scheme 60).[42] In their work, the abundant base-metal catalyst CpMn(CO)$_3$ was used, and it exhibited excellent position control. Particularly worth not-

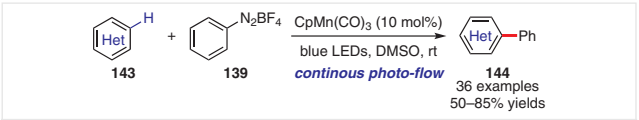

Scheme 60 Visible-light-driven, Mn-catalyzed C–H arylation of heteroarenes in a photo-flow manner

ing is that the first continuous photoflow strategy was reported for manganese-catalyzed C–H functionalizations, thus enabling efficient gram-scale synthesis and outperforming the corresponding batch approach.

A possible mechanism is illustrated in Scheme 61. First, ligand exchange and subsequent coordination by arenediazonium salt **139** delivers the complex **B**, which is transformed into its excited state **B*** under visible light illumination. Second, electron transfer of **B*** and radical addition to heteroarenes **143** affords intermediate **E**, which is converted into the final product **144** through further oxidation/deprotonation processes.

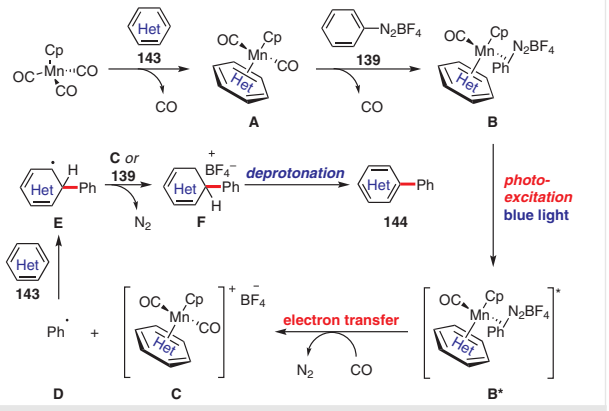

Scheme 61 Possible mechanism for the Mn-catalyzed C–H arylation of heteroarenes in a photo-flow manner

Visible-light-induced oxidative C–H acylation can also be successfully achieved without photocatalyst. In 2018, the Lei group developed a practical method for the acylation of N-heterocyclic aromatic compounds **145** with diverse aldehydes **99** (Scheme 62).[43]

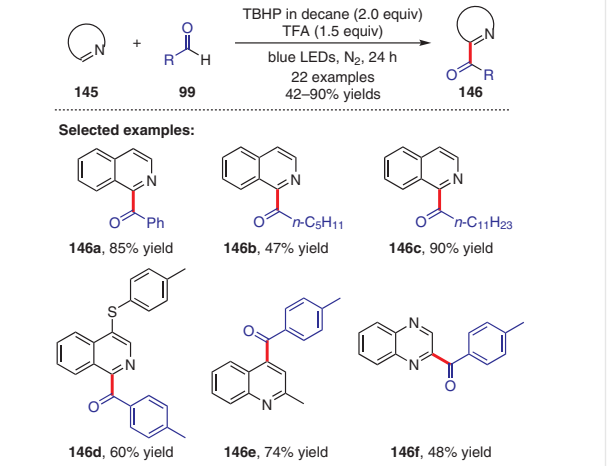

Scheme 62 Photoredox-induced Minisci coupling of N-heterocyclic aromatic compounds with aldehydes

A plausible mechanism for the oxidative coupling is proposed in Scheme 63. The reaction starts from the formation of a complex **B** in the presence of TFA and *tert*-butyl hydroperoxide (TBHP). On irradiation by blue LEDs, complex **B** is cleaved to give the *tert*-butoxy radical and a hydroxyl radical. Hydrogen atom transfer (HAT) together with radical addition to the protonated heteroarene afford the intermediate **D**, which is transformed into the final product **146a** via a SET process.

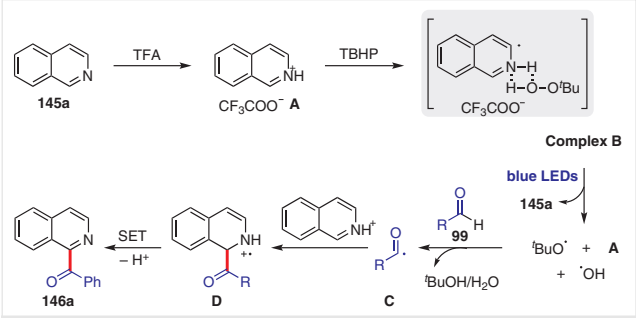

Scheme 63 Proposed mechanism for the Minisci coupling of N-heterocyclic aromatic compounds with aldehydes

Catalytic asymmetric photochemical reactions are a class of challenging research in modern synthetic chemistry. The Melchiorre group has performed elegant work in this area. They found that chiral enamines can participate in the photoexcitation of substrates selectively, achieving various asymmetric photochemical processes. In 2015, they demonstrated that the chiral electron-rich enamine can not only form an electron donor-acceptor (EDA) complex with electron-deficient substrates, but can also be transformed into its excited state by irradiation with visible light. This photo-organocatalytic strategy was applied to the enantioselective alkylation of aldehydes **147** and enals **149**, in combination with bromomalonates **148** to produce a variety of the alkylation products **151** and **152**, respectively, in high chemical yields and with excellent enantioselectivity (Scheme 64).[44]

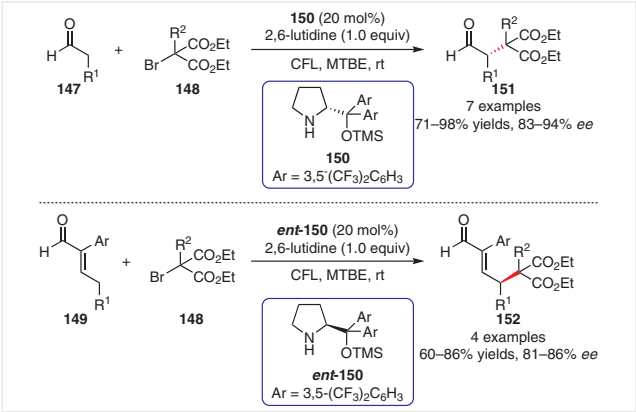

Scheme 64 Enantioselective alkylation of aldehydes and enals

A proposed mechanism is illustrated in Scheme 65. First, condensation of aminocatalyst **150** and butanal (**147a**) gives the enamine **A**. The ground state of this intermediate is excited to intermediate **A*** after absorbing visible light. Then, **A*** acts as an effective electron donor to reduce diethyl bromomalonate (**148a**), thus delivering radical **C**. Then, the radical alkylation of the enamine proceeds in a chain propagation pathway in a stereocontrolled fashion.

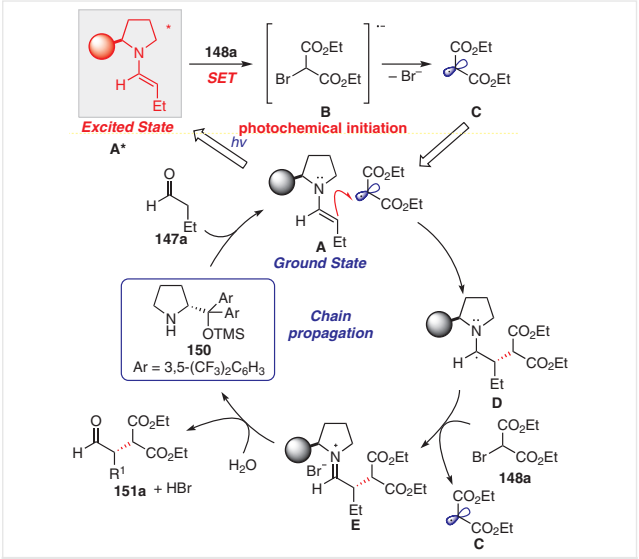

Scheme 65 Plausible mechanism for the enantioselective alkylation of aldehydes and enals

Motivated by these successful studies regarding the photochemical activity of enamines, the Melchiorre group further demonstrated that the excited state of chiral iminium ions can also exhibit great potential to make some reactions that are recalcitrant to thermal conditions feasible under visible light irradiation. They found that the asymmetric β-alkylation of enals **40** with alkylsilanes **153** was achieved when they were irradiated by visible light with chiral secondary amine **154** (TDS = thexyldimethylsilyl) as an effective organocatalyst (Scheme 66).[45] The reaction was conducted under mild conditions and gave the corresponding β-alkylated aldehydes **155** in good yields with broad substrate scope.

As shown in Scheme 67, in this reaction, the condensation of chiral secondary amine catalysts **154** and enals **40** affords iminium ions **A**, which reaches electronically excited state **A*** upon visible light excitation. This active species serves as a strong oxidant to furnish alkyl radical **B** and intermediate **C** in a SET process. At this juncture, a stereocontrolled intermolecular radical coupling gives enamine **D**, and subsequent hydrolysis forms the chiral product **155** while forging the stereogenic center at the same time. According to the results of quantum yield measurements and

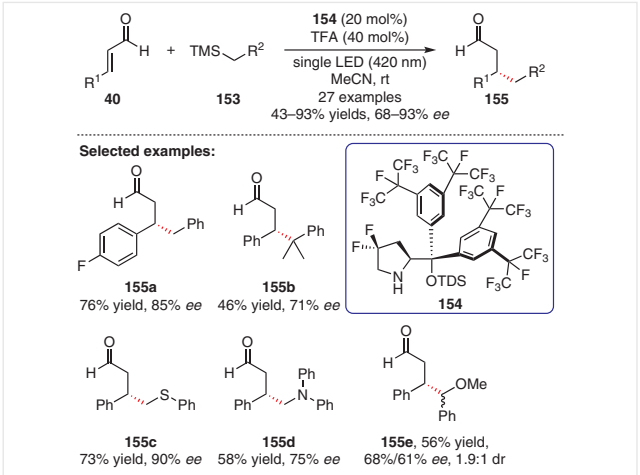

Scheme 66 Catalytic asymmetric β-alkylation of enals enabled by visible light excitation of iminium ions

literature reports, the authors speculated that the radical coupling mechanism is the dominant pathway compared to the radical chain propagation mechanism.

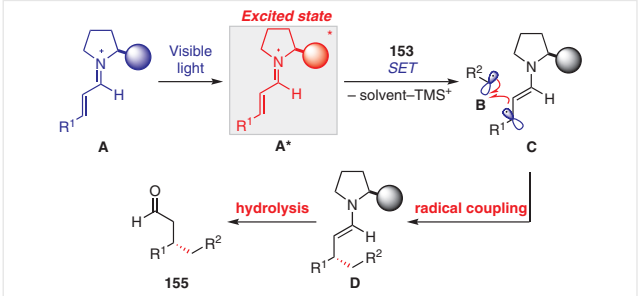

Scheme 67 Possible reaction pathway for the catalytic asymmetric β-alkylation of enals

In 2018, the Melchiorre group further applied this strategy to achieve asymmetric radical cascade reactions. It was found that, α,β-unsaturated aldehydes **40** and unactivated olefins **156** were easily converted into a variety of chiral compounds bearing butyrolactone or tetrahydrofuran skeletons **157** with excellent enantiocontrol (Scheme 68).[46] Additionally, a catalytic asymmetric three-component radical cascade reaction involving two intermolecular radical steps was feasible under established conditions.

Also in 2018 they reported a visible-light-induced direct C–H functionalization of toluene and xylene derivatives **158** by using chiral amine **159** as the catalyst (Scheme 69).[47] In this work, benzylic radicals were generated in a proton-coupled electron-transfer manner. The stereocontrolled radical coupling of benzylic radicals with a 5π-electron β-enaminyl radical intermediate yields the final products with high enantioselectivity.

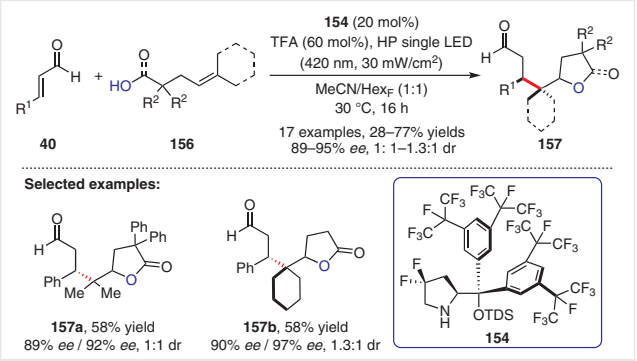

Scheme 68 Enantioselective radical cascade reactions

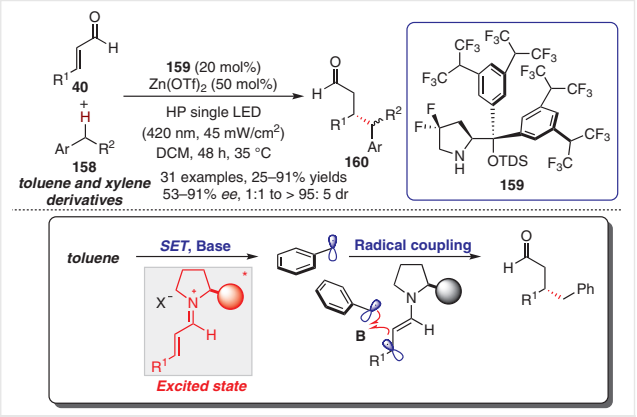

Scheme 69 Enantioselective C–H functionalization of toluene and derivatives

The Melchiorre group further exploited the potential of chiral organocatalytic intermediates for enantioselective photochemical cascade processes. This strategy directly converts α,β-unsaturated aldehydes **40** and racemic cyclopropanols **161** into stereochemically dense cyclopentanols **162** with exquisite stereoselectivity (Scheme 70).[48] Notably, the chiral secondary amine catalyst **159** controls both steps of the cascade process.

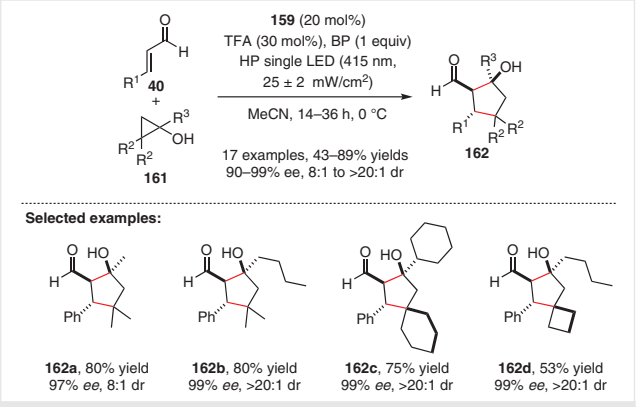

Scheme 70 Enantioselective photochemical organocascade catalysis of α,β-unsaturated aldehydes and racemic cyclopropanols

In 2019, the Melchiorre group exploited a nucleophilic dithiocarbamate anion catalyst **165**, which is modified with a chromophoric unit, to activate various alkyl electrophiles **163** (Scheme 71).[49] The generated radical adds to dimethyl fumarate (**164**) via an S_N2 pathway. The resulting photosensitive intermediate affords radicals upon homolytic cleavage induced by visible light. After the radical addition to fumarate and the subsequent H-abstraction from γ-terpinene, the desired conjugate addition products **166** were produced in high efficiency. This approach features mild conditions, a broad substrate scope, and excellent performance in the late-stage functionalization of marketed drugs.

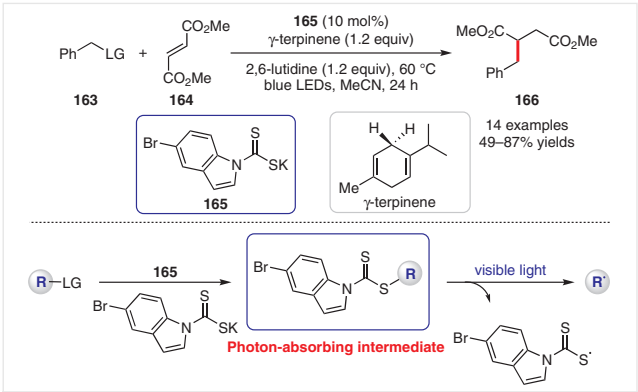

Scheme 71 Photochemical radical addition

As early as 2015, the Melchiorre group used their novel photochemical strategy to direct the aromatic perfluoroalkylation of phenols **167** using perfluoroalkyl iodides **90** as an effective fluoro source, giving the fluorinated adducts **168** in moderate to good yields (Scheme 72);[50] unsubstituted phenol or phenols bearing an electron-donating group were not suitable for this reaction. Notably, the perfluoroalkylated adducts of *meta*-aryl-substituted phenols exhibited axial chirality, and these moieties are important stereogenic elements found in several natural products. However, an asymmetric version with a chiral phase-transfer catalyst or a chiral base was unsuccessful. For the mechanism, similar to previous studies, the authors postulated that the key intermediate **A** was formed from the deprotonation of phenol **167** by 1,1,3,3-tetramethylguanidine (TMG). After illumination with visible light, anion **A** could reach excited state **A*** to create perfluoroalkyl radicals **B** from R_FI via a SET process. Finally, product **168** is provided via a classic homolytic aromatic substitution (HAS) pathway with the radical chain propagation mechanism.

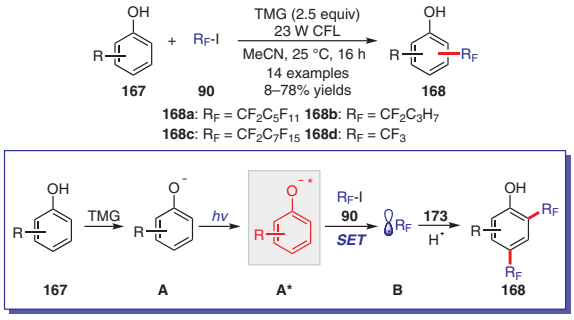

Scheme 72 Photochemical direct perfluoroalkylation of phenols

In 2018, Zhu and co-workers reported a photoirradiated regioselective intermolecular heteroarylation of unactivated alcohols, e.g. pentan-1-ol (**170**), with quinolines, e.g. 4-methylquinoline (**169**), to deliver the Minisci-type products **171** (Scheme 73).[51] In this reaction, phenyliodine bis(trifluoroacetate) (PIFA) is vital for realizing this challenging transformation.

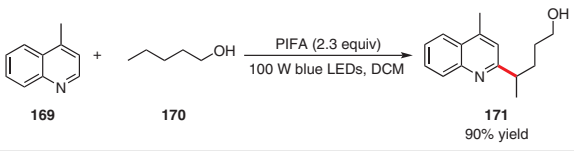

Scheme 73 Regioselective functionalization of remote unactivated C(sp^3)–H bonds

In addition to C–C bond formation, visible-light-induced photocatalytic approaches without a photocatalyst are also suitable for the construction of C–N bonds. In 2016, Peters, Fu, and co-workers reported a photoinduced copper-catalyzed approach for asymmetric C–N coupling, generating quaternary stereocenters with excellent enantiocontrol

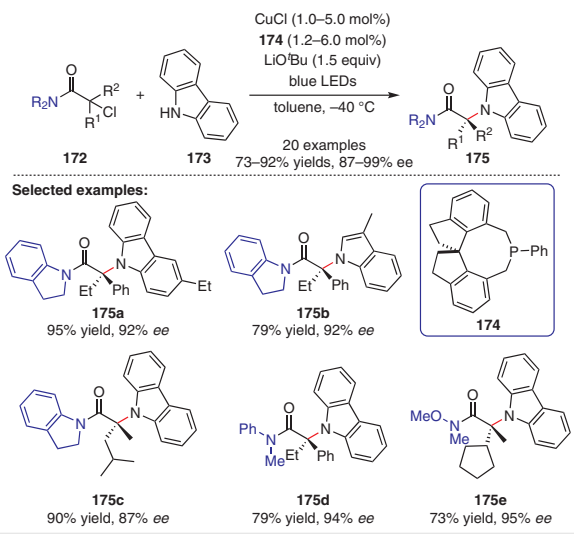

Scheme 74 Photoinduced copper-catalyzed C–N cross coupling

(Scheme 74).[52] In contrast to their earlier studies of UV-light-induced copper-catalyzed N-alkylations, this process operated under visible light from blue LEDs at relatively low catalyst loading. In this process, copper salts were responsible for both the photochemical profile and the enantiocontrolled bond formation. Under the optimized conditions, the protocol accommodated a wide range of *N*-acylindoline-derived electrophiles and substituted carbazoles, producing the corresponding C–N coupled adduct **175** in good to excellent yields.

A possible reaction mechanism is outlined in Scheme 75. The excitation of complex **A** with visible light provides an excited state adduct **B**, which undergoes single electron transfer with the alkyl halide **172** to deliver an alkyl radical. The radical then combines with copper(II)–nucleophile complex **C**. After reductive elimination, the desired coupling product **175** is produced smoothly along with the intermediate **D**; the latter is converted into complex **A** through ligand substitution with nucleophile to participate in the catalytic cycle.

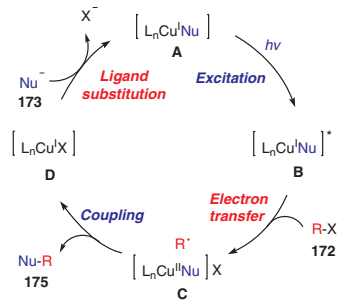

Scheme 75 Proposed mechanism for photoinduced copper-catalyzed C–N cross coupling

Since 2012, the Hwang group has developed a range of photoinduced cross-coupling and C–H annulation reactions catalyzed by CuCl at room temperature.[53] For example, in 2015 they reported a CuCl-catalyzed multicomponent coupling under irradiation with visible light (Scheme 76).[53c] This method provides an efficient and atom-economical

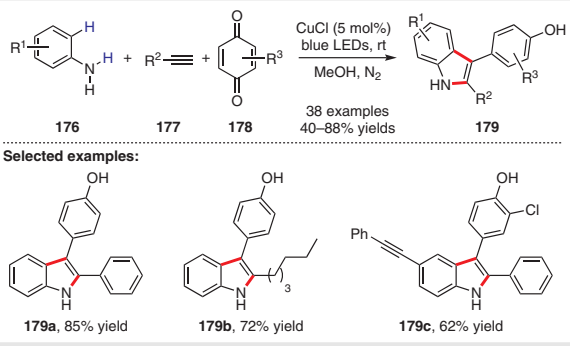

Scheme 76 Photoinduced copper-catalyzed regioselective synthesis of indoles

methodology for the preparation of indole derivatives **179** from easily accessible starting materials under relatively mild conditions. Notably,this approach shows great advantages for circumventing the formation of homocoupling byproducts that are common in Cu-catalyzed oxidative annulation involving terminal alkynes.

To study the mechanism, EPR measurements, cyclic voltammetry, and additional control experiments were conducted. According to the results of luminescence quenching experiments, benzoquinone was suggested to be responsible for quenching the excited state of the copper(I) phenylacetylide. A plausible mechanism is proposed in Scheme 77. First, illumination of in situ generated copper intermediate **A** by blue LEDs produces photoexcited **A***, which undergoes a SET process with benzoquinone **178a** to give the radical anion **C** and the copper(II) phenylacetylide **B**. Then, radical anion **C** addition to the intermediate **B**, and a reductive elimination regenerates CuCl and **D**, which is attacked by aniline with the assistance of CuCl to provide complex **F**. Finally, cyclization of **F** followed by aromatization generates indole product **179a**.

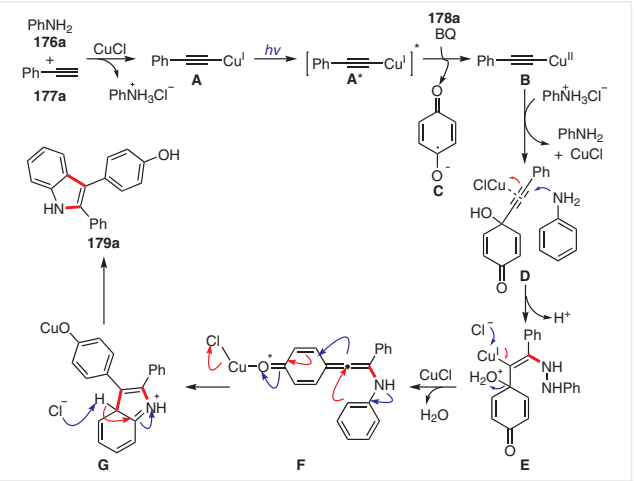

Scheme 77 Proposed mechanism for the photoinduced copper-catalyzed regioselective synthesis of indoles

In 2017, Wu, Liu, and co-workers accomplished a visible-light-induced, copper salt catalyzed construction of thiazoles **182** without a photocatalyst (Scheme 78).[54] In this process, the generated $Cu(NCS)_2^-$ plays a dual role as both photosensitizer and Lewis acid. Under the optimized conditions, various vinyl azides with different functional groups were all well tolerated. Notably, the ammonium cation was necessary to provide a proton in this transformation.

According to the results of mechanistic investigation including UV-visible absorption, HRMS analysis, IR monitoring, and radical trapping experiments, a mechanism involving energy transfer is described in Scheme 79. Photoactivation of $Cu(NCS)_2^-$ **A** produces its excited state **A***, which

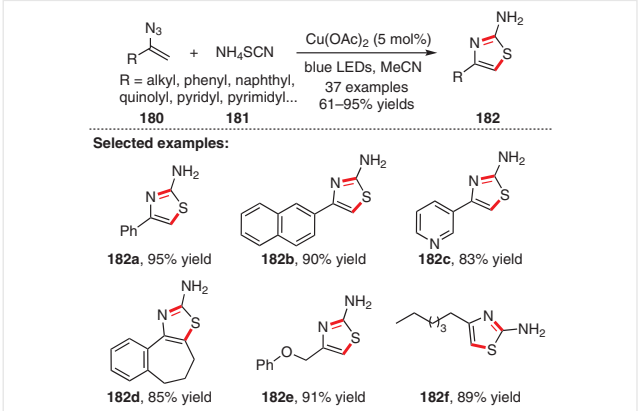

Scheme 78 Visible-light-driven construction of thiazoles

induces the generation of 2*H*-azirines **B** via an energy transfer pathway. Lewis acid activated intermediate 2*H*-azirines **C** then undergo nucleophilic ring opening with thiocyanide providing intermediate **D**. Finally, intramolecular annulation followed by protonation generates the desired 2-aminothiazoles **182**.

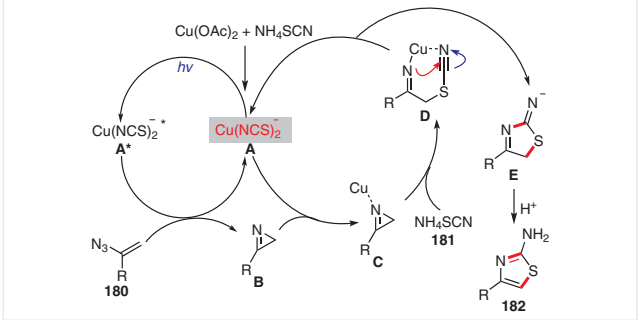

Scheme 79 Proposed catalytic cycle for the construction of thiazoles

In 2017, Wu and co-workers reported a visible-light-induced, Cu(II)-catalyzed C–H bond functionalization of secondary amines **183** with indoles **184**, arylacetylenes **185**, β-keto ester derivatives **186**, and β-diketone derivatives **187** (Scheme 80).[55] A series of mechanistic experiments and DFT calculations were conducted to identify the key intermediates. The data suggested that the new species of Cu(II) salts associated with secondary amines can absorb visible light, which enables this photocatalyst-free photochemical transformation.

Sequential Au catalysis and photoactivation for the construction of indoles was developed by D. Z. Wang and coworkers. In the presence of Gagosz's catalyst PPh_3AuNTf_2 and visible light irradiation, the protocol accommodated a wide range of substituted anilines **192** and alkynes **193**, producing the corresponding functionalized indoles **194** in excellent yields (Scheme 81).[56] A plausible mechanistic rationale is briefly depicted. Dual Au/Mg Lewis acidic activation of **193** triggers hydroamination addition of anilines

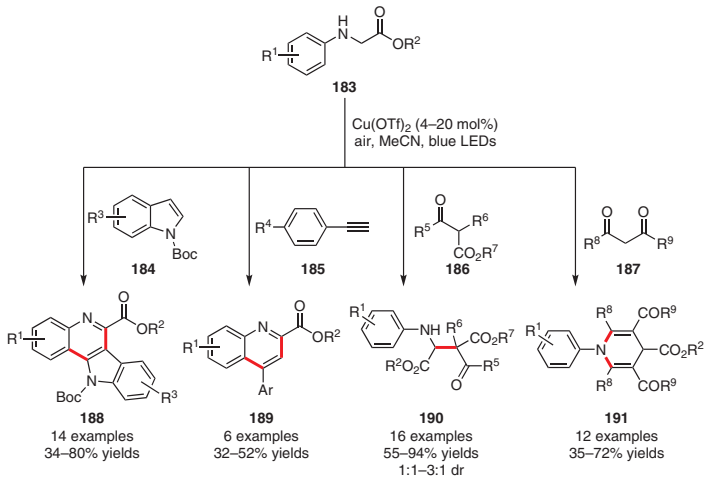

Scheme 80 Visible-light-driven C–H functionalization

192 to give an enamine species **A**, which then undergoes photoexcitation to its excited state **A***. Subsequent radical cyclization and single electron transfer yields the indole product **194**.

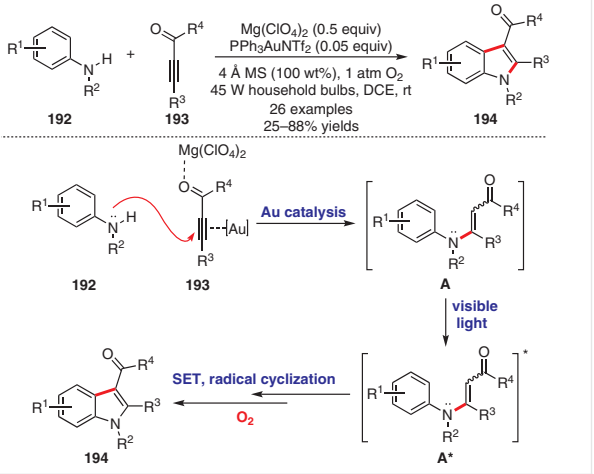

Scheme 81 Sequential catalysis for the synthesis of indoles

An efficient method for synthesizing pyrazoles **196** through a sunlight-induced annulation of hydrazones has been developed by Zhu and co-workers (Scheme 82).[57] Based on the results of mechanism investigation, the reaction was believed to proceed via irradiation of anion intermediate **A** with sunlight to generate excited state **A***, from which single-electron transfer gives the N-centered radical **B**. Finally, an intramolecular annulation of radical **B** affords the desired pyrazole product **196**.

In 2018, Che, Yu and co-workers discovered that the C–P bond can be efficiently forged by employing heteroaryl halides **197** and diarylphosphine oxides **198** as substrates. Notably, this reaction can proceed smoothly without transition metals or photocatalysts, just requiring visible light irradiation (Scheme 83).[58]

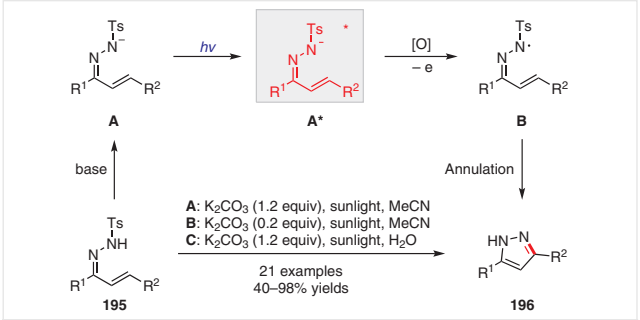

Scheme 82 Sunlight-promoted direct irradiation of α,β-unsaturated hydrazones for pyrazole synthesis

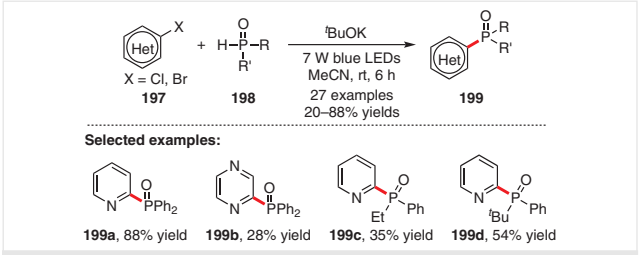

Scheme 83 Phosphinylation of heteroaryl halides

4 Visible Light Photoexcitation of EDA Complexes between Substrates

Organic synthesis involving the formation of photosensitive electron donor-acceptor (EDA) complexes has grown rapidly due to the advantages of mild conditions and satisfactory functional group tolerance. In this section, visible-

light-induced organic transformations based on EDA complex formation between two substrates are summarized. In 2011, the MacMillan group developed the visible light photoredox catalyzed trifluoromethylation of enol silanes (Scheme 84).[59] In addition to ketone-derived enol silanes, other substrates, such as silyl ketene acetals and *N*,*O*-acetals derived from esters and amides, also afforded the trifluoromethylation products. Notably, this reaction could occur without photoredox catalysts. The authors assumed that an EDA mechanism was likely operative, but they did not provide experimental evidence.

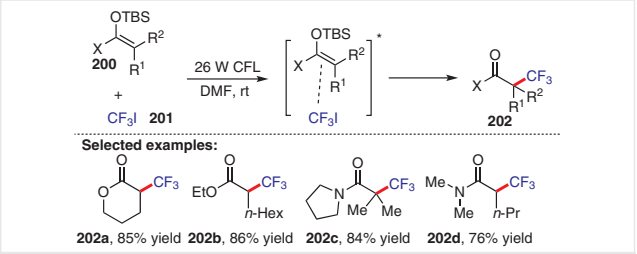

Scheme 84 Visible-light-driven trifluoromethylation of enol silanes

In 2013, Chatani and co-workers reported a visible-light-driven photoredox arylation of arenes and heteroarenes with diaryliodonium salts as aryl radical precursors (Scheme 85).[60] It was interesting to find that pyrroles, unlike other heteroarenes, participated without a photocatalyst in the presence of visible light. In the mechanistic studies, a new absorption band attributed to the formation of a colored charge-transfer (CT) complex was discovered during the UV-vis spectroscopic analysis of the reaction mixture. In this EDA photoactivation process, an EDA complex that is generated between pyrroles **203** and diaryliodonium salts **204** is sensitized with visible light lumination to generate intermediate **A** and phenyl radical **B**; after radical recombination and deprotonation, the desired product is obtained.

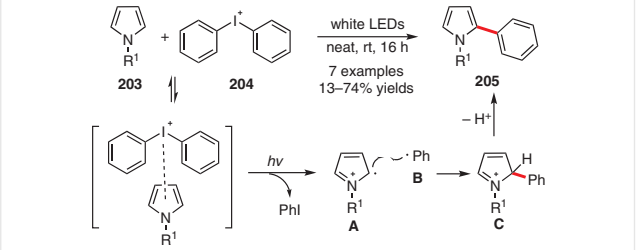

Scheme 85 Visible-light-driven arylation of arenes and heteroarenes

In 2015, the Melchiorre group developed indole alkylation via the photoactivation of EDA complexes generated between indoles **206** and electron-deficient benzyl or phenacyl bromides **207**.[61a] Herein, they successfully isolated a stable dark-orange crystal of the EDA complex and obtained complete characterization by X-ray single-crystal spectroscopic analysis. The X-ray structure confirmed the formation of an EDA complex with a 1:1 donor–acceptor ratio, which was in accord with the results of Job's method. To elucidate the role of the EDA complex, a series of control experiments were conducted, which indicated that the photoactivity of the EDA complex was solely responsible for the reaction. Regarding the substrate scope, in addition to electron-deficient benzyl bromides, various phenacyl bromides participate in the reaction effectively. Moreover, 2,3-disubstituted 1*H*-indoles also provided valuable indolenine products through a dearomatization pathway.

In the proposed catalytic cycle, the radical pair **A** and **B** is formed upon irradiation of the EDA complex. Then, radical combination within a solvent cage and subsequent aromatization yields the desired product (Scheme 86).

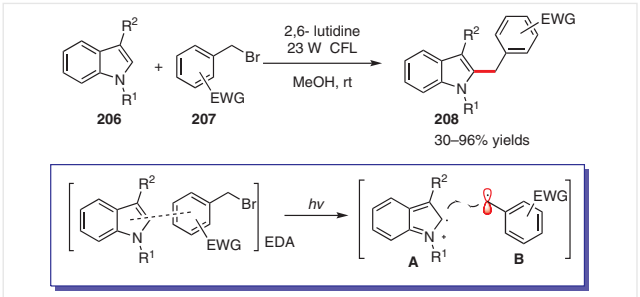

Scheme 86 Alkylation of indoles via photoactivation of EDA complex

Inspired by this work, in 2018 the You group developed a visible-light-driven intramolecular dearomatizative reaction of indole derivatives (Scheme 87).[61b] It is believed that indole derivatives **209** and Umemoto's reagent **210** form a photosensitive EDA complex; without photocatalysts, a variety of spiroindolenines bearing a quaternary stereogenic center **211** were accessed in good yields.

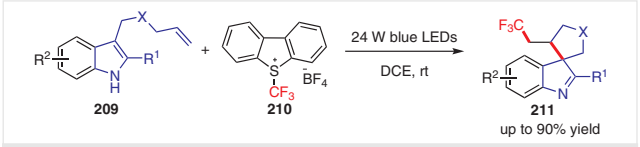

Scheme 87 Intramolecular dearomatization of indole via the photoactivation of EDA complexes

In 2015, the Paixão group described a visible-light-induced intramolecular reductive cyclization, providing an efficient method for preparing oxindoles **214** and indoles **216** (Scheme 88).[62] In this reaction, the EDA complex generated from the association of functionalized anilines and tris(trimethylsilyl)silane (**213**, TTMSS) was the key intermediate. Under the optimized conditions, variation of the electronic properties of the substituents does not obviously affect the efficiency of the reaction.

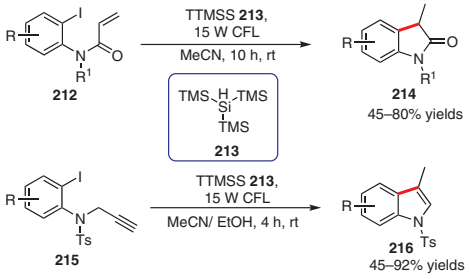

Scheme 88 Photochemical method for the synthesis of indoles and oxindoles

A possible reaction pathway is illustrated in Scheme 89. The visible-light-promoted excitation of the EDA complex, which is formed through the association of aryl substrates with TTMSS **213**, enables the energy transfer to silane **213**, generating the Si-based radical **A**. Then, reduction of the substrate **215** by intermediate **A** provides aryl radical **B**. Next, the radical **B** undergoes a 5-*exo*-dig cyclization and hydrogen abstraction leading to the formation of final product **216**.

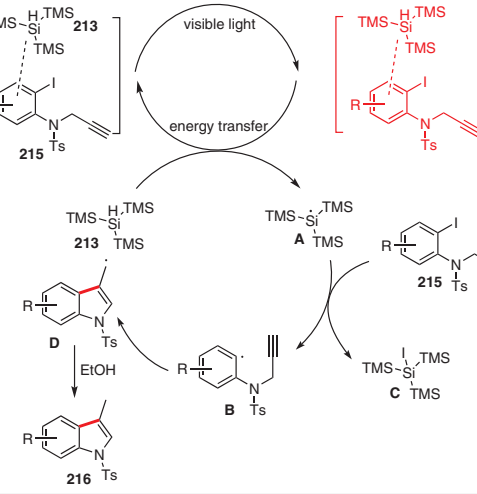

Scheme 89 Visible-light-promoted intramolecular reductive cyclization

In 2015, Zeitler and co-workers reported visible-light-driven dehydrogenative cross-coupling reactions in the absence of an external photocatalyst.[63] In this protocol, the tetrahydroisoquinolines **217** were oxidized with $BrCCl_3$ under illumination to give the corresponding iminium ion intermediates **218**, which further reacted with different types of nucleophiles to obtain the final dehydrogenative coupling products **220** (Scheme 90).

Based on the results of mechanistic investigations including in situ infra red and cyclovoltammetric measurements, two reaction pathways were proposed. One is visible-light-induced homolytic cleavage, and the other involves the photoactivation of the EDA complex. Herein, we

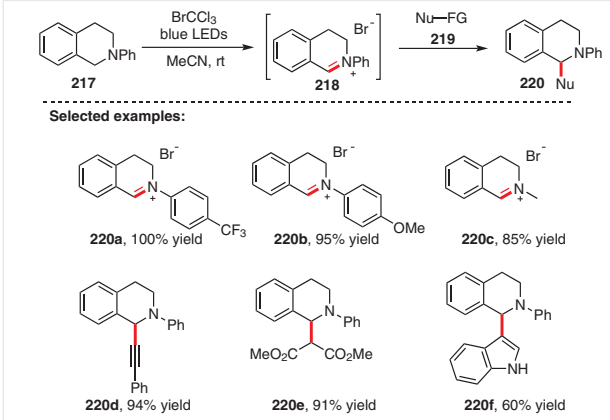

Scheme 90 Visible-light-induced dehydrogenative coupling

focus on the EDA mechanism. As depicted in Scheme 91, the mechanism involving EDA complex formation starts with electron transfer enabled by the activation of the EDA intermediate under visible light. The generated radical cation **A** releases a proton to afford radical **B**, which forms the iminium ion intermediates **218** via an atom transfer or oxidation process.

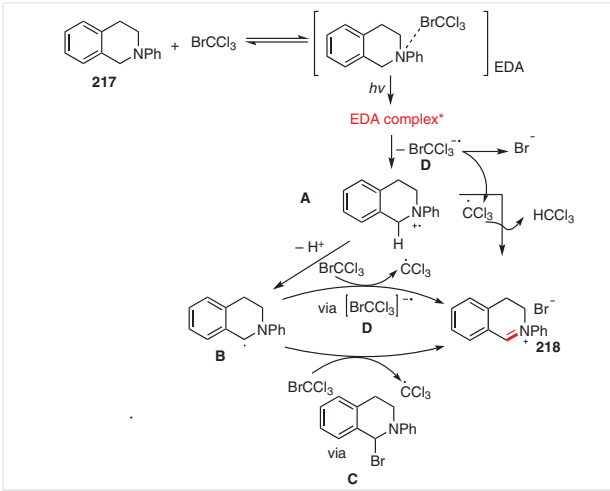

Scheme 91 Proposed mechanism for visible-light-induced dehydrogenative coupling

Also in 2015, Leonori and co-workers developed a visible-light-mediated hydroimination and iminohydroxylation cyclization.[64a] Interestingly, iminohydroxylation cyclization proceeded efficiently without a photocatalyst. This reaction was promoted by the photoactivation of an EDA complex generated between an electron-deficient aryloxy group and triethylamine. Under catalyst-free conditions, the iminohydroxylation products **222** were obtained exclusively by excluding cyclohexadiene from the reaction mixture. In addition, they confirmed the existence of an

EDA complex and a stoichiometric ratio of electron-acceptor **221** to electron-donor triethylamine of 1:1 using UV-vis spectroscopy and Job's method (Scheme 92).

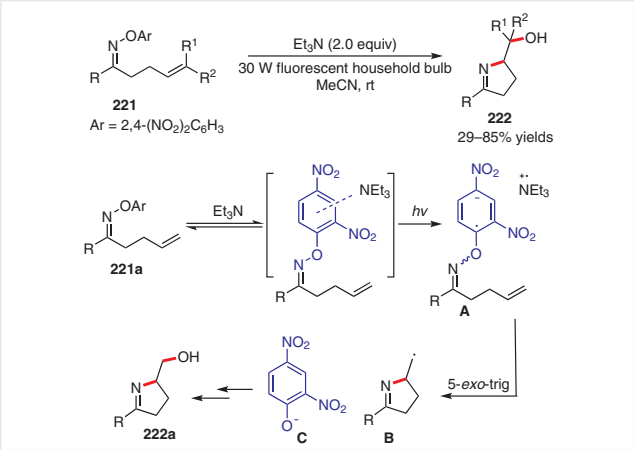

Scheme 92 Visible-light-mediated iminohydroxylation cyclization

Using this strategy, nitrogen-centered radicals can be generated easily under relatively mild conditions without a photocatalyst, providing convenient access to various nitrogen heterocycles. For example, inspired by this research, the Fu group designed an intramolecular C(sp^3)–H imination of amines containing the same aryloxy group.[64b] In their work, 2,4-dinitrophenol, the byproduct of the reaction, acted as an oxidant during the oxidation process (Scheme 93). The Wu group applied this strategy to the field of sulfur dioxide insertion reactions, successfully achieving aminosulfonylation of the C(sp^3)–H bond.[64c] In addition to aminosulfonylation of unactivated C(sp^3)–H bonds, substrates **228** containing benzyl C(sp^3)–H bonds also showed great reactivity under standard conditions (Scheme 94). They also developed an N-radical-involving cyclization with the insertion of SO_2 under photoinduced and photocatalyst-free conditions.[64d] The reaction featured high efficiency, good selectivity, and broad functional group tolerance. Both of these reactions proceed via the photoactivation of an EDA complex composed of aryl oximes and DABCO·$(SO_2)_2$. In 2018, the Manolikakes group also successfully achieved the visible-light-induced synthesis of sulfonylated oxindoles via the formation of an EDA complex between DABCO·$(SO_2)_2$ and iodonium salt.[65a]

Iodonium salts usually act as electron acceptors in the formation of EDA complexes. For example, Lakhdar and co-

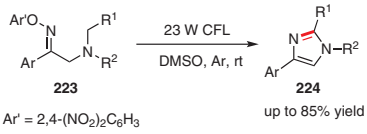

Scheme 93 Visible-light-induced intramolecular imination

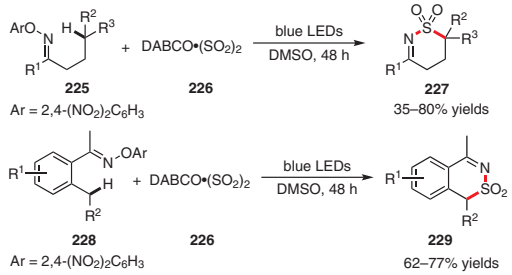

Scheme 94 Visible-light-mediated aminosulfonylation

workers utilized Ar_2I^+ as an aryl radical precursor to form an EDA complex with phosphites **231**.[65b] Using this practical and simple approach, a variety of arylphosphonates were synthesized in moderate to good yields. Notably, the UV-vis spectrum of the EDA complex did not show a bathochromic effect, which may be attributed to thermodynamically unfavorable association of Ar_2I^+ and phosphites to form a low concentration of a weak EDA complex (Scheme 95).

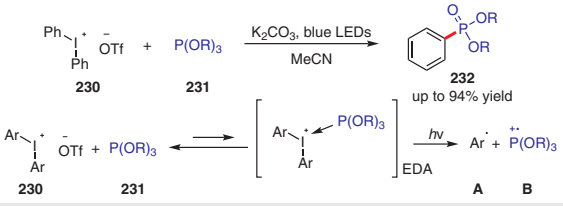

Scheme 95 Visible-light-mediated synthesis of arylphosphonates

In 2016, the Ragains group reported a novel photoreaction for *O*-glycosylation with a thioglycoside in the absence of photocatalyst (Scheme 96).[66] Under optimal reaction conditions involving illumination with blue LEDs, a wide range of alcohol acceptors were functionalized using Umemoto's reagent **234** to produce glycosylation products **235** in moderate to high yields. According to the color change of Umemoto's reagent **234** and *p*-methoxystyrene in MeCN and other mechanistic experiments including radical trapping, EPR spectroscopic analysis, and DFT calculations, the EDA complex composed of Umemoto's reagent **234** and *p*-methoxystyrene moiety of **233** was a prerequisite for photon absorption.

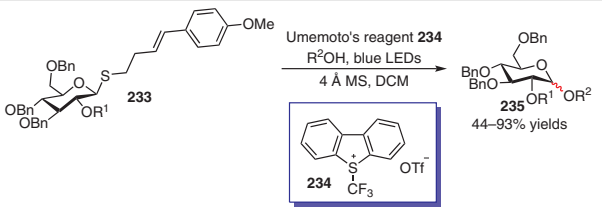

Scheme 96 Visible-light-promoted *O*-glycosylation

In 2017, the Dilman group reported a radical silyldifluoromethylation of electron-deficient alkenes **237** assisted by an NHC·borane complex affording the silyldifluoroalkanes **239** in moderate to high yields (Scheme 97).[67] A wide range of electron-deficient alkenes with useful functional groups were suitable for this transformation. Control experiments with a light/dark sequence indicated a possible mechanism involving a radical chain pathway.

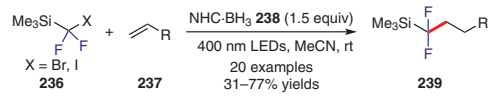

Scheme 97 Radical silyldifluoromethylation of electron-deficient alkenes

As depicted in Scheme 98, an EDA complex is formed between silane **236** and NHC·borane **238**, which is stabilized by halogen–hydride interaction. Upon irradiation with visible light, this complex undergoes homolytic fragmentation, producing radical **A** to initiate the reaction. The generated radical **A** is added to alkene **237**, forming radical intermediate **B**. Then, **B** abstracts a hydrogen from NHC·borane **238** to provide another radical **C** and product **239**. Radical **C** abstracts the halogen atom from substrate **236** to regenerate radical **A** and form the haloborane byproduct **D**.

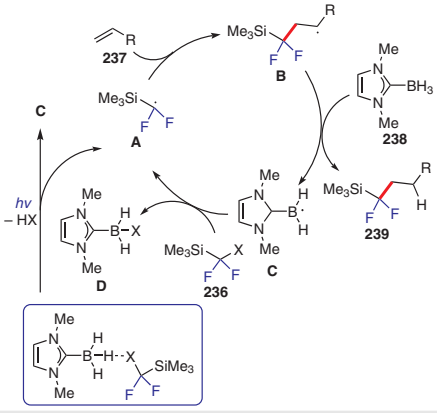

Scheme 98 Proposed mechanism for the silyldifluoromethylation of electron-deficient alkenes

In 2016, Ma, Yu, and co-workers reported a halogen bond (XB) enabled visible-light-irradiated isocyanide insertion.[68a] The EDA complex was clearly verified by ^{19}F NMR titration experiments and Job's method. A visible-light-induced electron transfer enables the generation of R_F radical **A**, providing a variety of 2-fluoroalkylated quinoxalines **241** after double radical isocyanide insertion steps (Scheme 99).

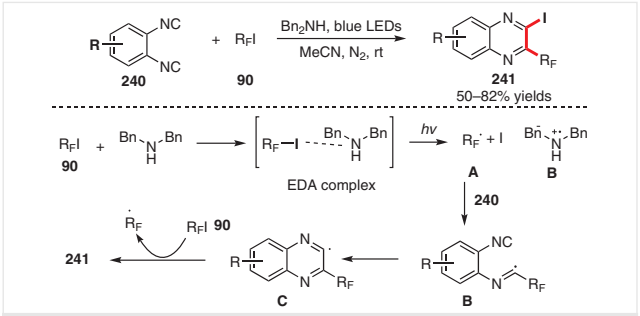

Scheme 99 Visible-light-irradiated halogen bond (XB) promoted isocyanide insertion

In 2017, the Studer group reported a visible-light-induced difunctionalization of alkenes via radical migration (Scheme 100).[68b] Similarly, the reaction is believed to be initiated by photoactivation of an EDA complex, which is formed between perfluoroalkyl iodide **243** and DABCO.

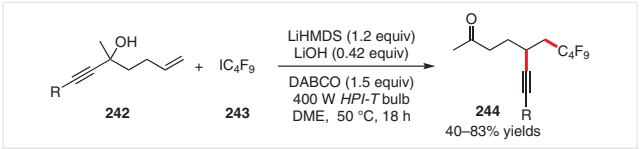

Scheme 100 Halogen bond (XB) promoted α-perfluoroalkylation/β-alkynylation reactions under visible light irradiation

In 2017, a visible-light-promoted arylation of anilines with heteroaryl halides was reported by the König group.[69] Notably, heteroaryl halides bearing electron-withdrawing groups are necessary for formation of an EDA complex with anilines **246** (Scheme 101).

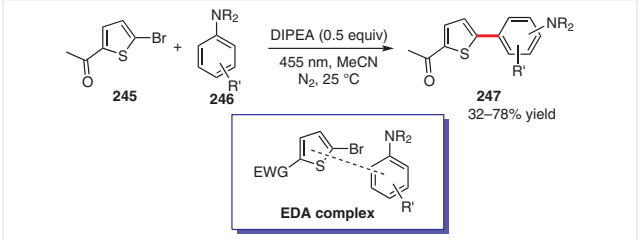

Scheme 101 Radical arylation of anilines

In 2017, the Chen group disclosed the first EDA complex enabled, visible-light-driven alkoxyl radical generation.[70] Under standard conditions, an array of linear primary, secondary, and tertiary *N*-alkoxyphthalimides were tolerated in this reaction. Based on mechanistic investigations, a possible reaction pathway is depicted in Scheme 102. The photoinduced single electron transfer within the EDA complex generated between Hantzsch ester **33** and *N*-alkoxyphthalimides **248** formed the *N*-alkoxyphthalimide radical an-

ion **A**. After releasing phthalimide, the alkyl radical **E** is obtained, which is further trapped by allyl sulfones **249** to give the desired products.

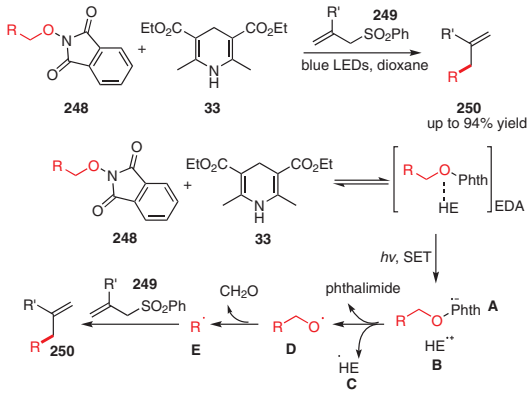

Scheme 102 Visible-light-promoted alkoxyl radical generation for the radical allylation reaction

5 Visible Light Photoexcitation of EDA Complexes between Substrates and Reaction Intermediates

In 2013, the Melchiorre group reported an unprecedented enantioselective α-alkylation of aldehydes through the visible-light sensitization of EDA complexes (Scheme 103).[7] They found that the chiral enamine generated from condensation between aldehyde **251** and chiral secondary amine **253** further combined with electron-acceptor **252** to form a photon-absorbing chiral EDA complex. As for the substrate scope, aldehydes having sterically hindered chains or heteroatom moieties were well tolerated in this reaction. Moreover, all-carbon quaternary stereocenters could be constructed with high fidelity, which is extremely difficult to achieve in thermal reactions. Based on control experiments and mechanistic studies, the pathway involving out-of-cage radical diffusion and chain propagation was ruled out.

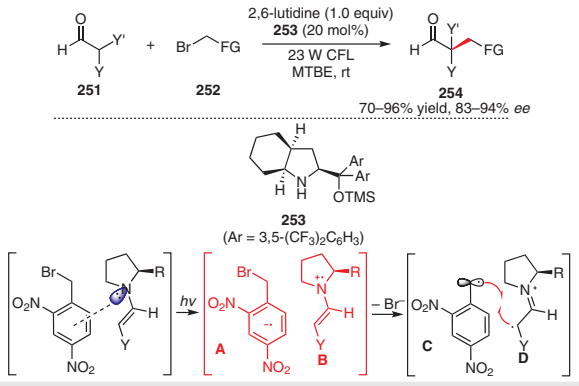

Scheme 103 Photoinduced enantioselective α-alkylation of aldehydes

In 2014, the Melchiorre group extended the strategy to the α-alkylation of ketones, as shown in Scheme 104.[71] Unlike the previous work, chiral secondary amines failed to promote the reaction, whereas the chiral primary amine **256** showed great reactivity in this reaction. In terms of substrate scope, a variety of cyclohexanones were used in the asymmetric alkylation reaction, moreover, five- and seven-membered cyclic ketones were competent substrates for this protocol.

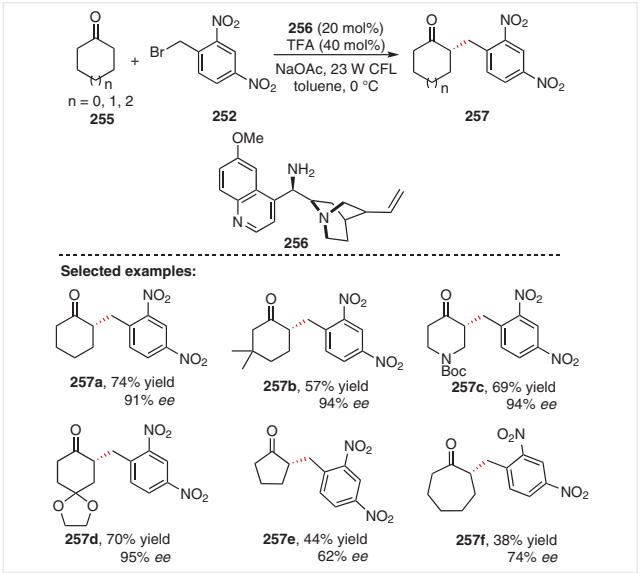

Scheme 104 Photoinduced asymmetric intermolecular α-alkylation of ketones

Also in 2014, the Melchiorre group successfully found that in situ generated enolates acted as electron donors to form an EDA complex instead of enamine species.[72] Control experiments indicated that the visible-light-induced photoactivation of the EDA complex formed between enolates **A** and perfluoroalkyl iodides **90** was responsible for the reactions. Generally, substrates with electron-withdrawing groups showed reduced efficiency compared with substrates bearing electron-donating groups due to the reduced electron density on the arene. Notably, the electronic properties of the EWGs at the benzylic moiety were crucial for the formation of the enolates and the ensuing C–C bond

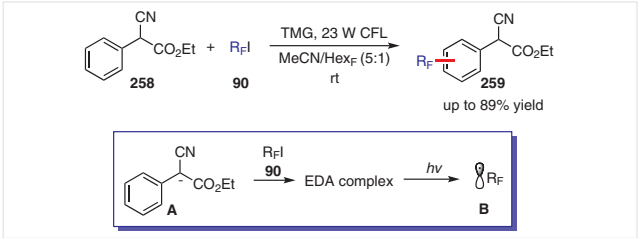

Scheme 105 Photoinduced aromatic perfluoromethylation

construction. This reaction has the advantage of simple operation and a broad substrate scope (Scheme 105).

In 2015, the Melchiorre group reported a photo-organocatalytic enantioselective prefluoroalkylation of β-keto esters (Scheme 106).[73] In this reaction, the chiral enolate **B** generated with the assistance of base and PTC served as an electron donor for EDA complex formation. With this method, an array of valuable products bearing chiral R_F-containing quaternary centers was constructed with high efficiency and stereoselectivity. Control experiments suggested that light, PTC catalyst, and Cs_2CO_3 were necessities for this reaction. Based on mechanistic studies and previous reports, a possible catalytic cycle is described here. Initially, the photoactivation of the EDA complex formed upon the complexation of chiral enolate **B** and R_FI **90** allows electron transfer to provide R_F radical **A**. Trapping this electron-deficient radical by chiral enolate **B** and subsequent iodine atom abstraction gives intermediate **D** and R_F radical **A**, then, **D** collapses to release product **262** (Scheme 106).

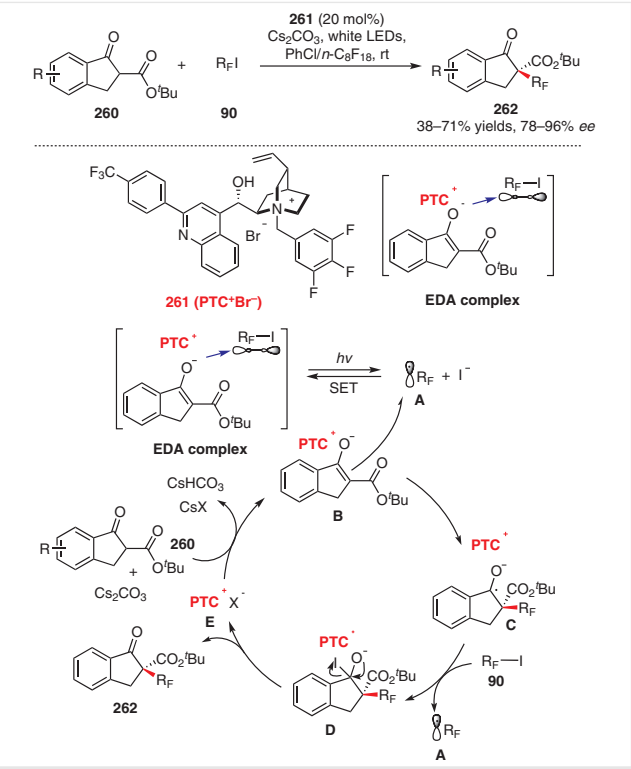

Scheme 106 Photochemical enantioselective perfluoroalkylation of β-keto esters

In 2016, the Yuan group reported the KOH/DMSO-promoted visible-light-induced synthesis of 2-substituted benzothiophenes (Scheme 107).[74] Notably, they found that an orange-red substrate was formed when 2-iodothioanisole (**263**) was added to the KOH/DMSO two-phase system. Based on electron spin resonance (ESR) and HRMS experiments, a visible-light-driven SET process from KOH/DMSO to 2-iodothioanisole is proposed.

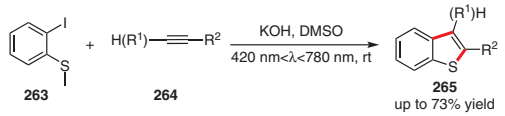

Scheme 107 Visible-light-induced synthesis of 2-substituted benzothiophenes

In 2017, Xiao, Chen and co-workers reported a photocatalytic generation of aza-*ortho*-quinone methides (aza-*o*-QMs), providing access to structurally diverse and densely functionalized indoles (Scheme 108).[75] The reaction proceeded without photocatalyst, indicating that a photoactive EDA aggregation might be involved in the process. This assumption was further confirmed by the color change upon the mixture of reagents and a bathochromic-shift of UV-vis absorption spectra. Under the standard conditions, acyl sulfur ylides bearing heteroaryl and cycloalkyl groups were well tolerated in the cascade reaction. Moreover, other radical sources proved to be valid in this reaction, however, in these cases, photocatalysts were necessary for the generation of the corresponding alkyl radicals and aza-*o*-QMs.

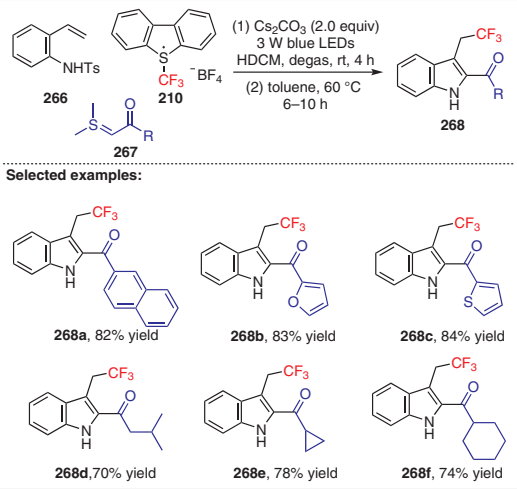

Scheme 108 Photocatalytic generation of indoles

A plausible mechanism is proposed for this multicomponent cascade reaction (Scheme 109). After deprotonation of **266** with base, the generated intermediate **A** associates with Umemoto's reagent **210** to form the photon-absorbing EDA complex, and electron transfer occurs under illumination to form trifluoromethyl radical **B**. This radical is trapped by substrate **266** to provide radical intermediate **C**, which is further oxidized by Umemoto's reagent through radical chain propagation. With the assistance of base, the key intermediate aza-*o*-QMs is formed. At this stage, a for-

mal [4+1] cycloaddition between aza-*o*-QMs **E** and sulfur ylide **267** followed by aromatization occurs to give the corresponding indoles.

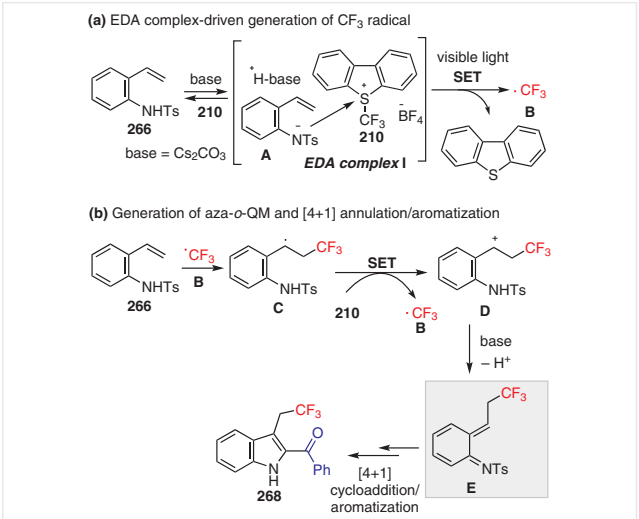

Scheme 109 Proposed mechanism for the photocatalytic generation of indoles

In 2017, Miyake and co-workers described visible-light-mediated C–S cross coupling without external photocatalyst (Scheme 110).[76a] EDA formation between thiolate anion and aryl bromide and subsequent electron transfer under illumination were the key steps of this transformation; the importance of these steps are also supported by DFT calculations. This reaction has attracted wide interest from synthetic chemists for its mild conditions and broad substrate scope. It is worth highlighting that the alkanethiols and arenethiols bearing different functional groups were tolerated under the optimized conditions. Moreover, some products

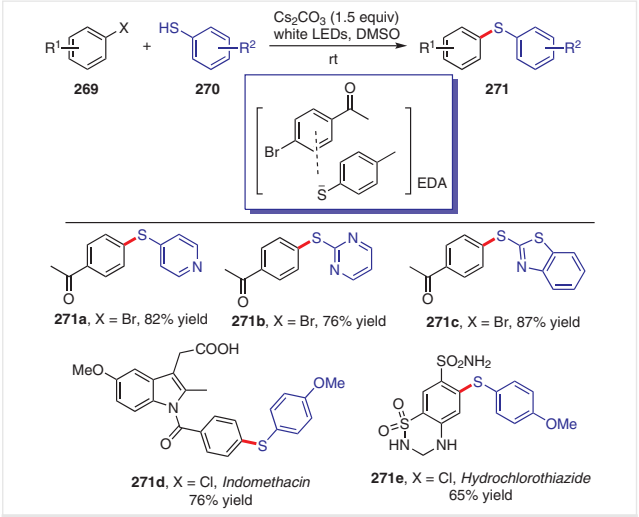

Scheme 110 Visible-light-mediated C–S cross coupling

were obtained efficiently with sunlight irradiation. To show the great synthetic potential of this method, the late-stage functionalization of various pharmaceuticals was conducted in good yields.

In 2018, Miyake and co-workers further presented the new reactivity of ethynylbenziodoxoles and ethynylbenziodoxolones **272**, which when reacted with phenols **167** afforded various (*Z*)-2-iodovinyl phenyl ether derivatives **273** under visible light irradiation; phenoxide was used as an electron donor in EDA complexes.[76b] A set of experiments and DFT calculations were performed to provide evidence that visible-light-driven one-electron reduction of vinylbenziodoxolone is the reason for Ph–I bond cleavage to furnish the final product (Scheme 111).

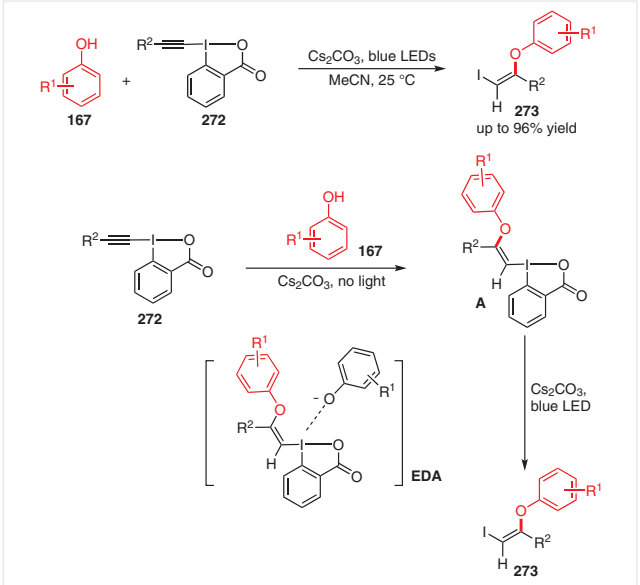

Scheme 111 Visible-light-induced C–O bond formation

In 2018, Miao, Wang, and co-workers reported a photodriven synthesis of C6-polyfunctionalized phenanthridines via a radical cascade reaction (Scheme 112).[77] The reaction was triggered through a photosensitization of EDA complexes that were generated from arylsulfinate anions and biaryl isocyanides. Notably, under blue light and UV light irradiation, *E*- and *Z*-products were obtained with high regio- and stereoselectivity, respectively.

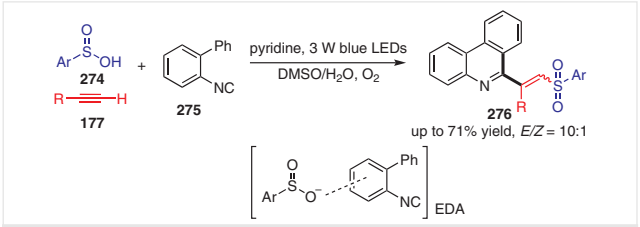

Scheme 112 Photoinduced construction of phenanthridines

Similarly, Guo, Chen, Fan, and co-workers developed a photoactivated three-component cascade annulation in the absence of photocatalyst affording a direct access to 2-iminothiazolidin-4-ones **280** with high efficiency (Scheme 113).[78] Key to this reaction is the in situ generation of H-bonding EDA complexes that are proposed based on the results of UV-vis spectroscopic measurements.

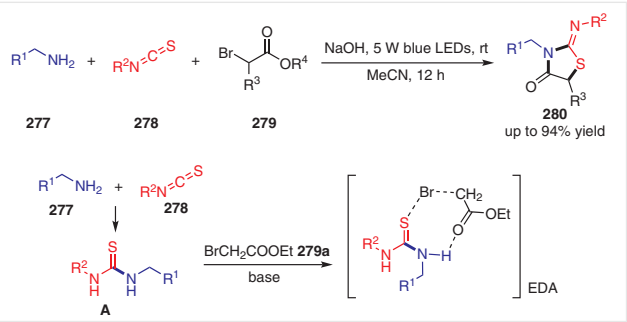

Scheme 113 Photo-driven three-component tandem annulation

In 2018, the Aggarwal group developed a deaminative borylation, conducted via the formation of an EDA complex between *N*-alkylpyridinium salts **281** and an adduct between B_2cat_2 **82** and DMAc.[79] This approach features simple operation, mild conditions, and excellent function group tolerance. Moreover, several complex natural products can be functionalized with high diastereoselectivities through this approach (Scheme 114).

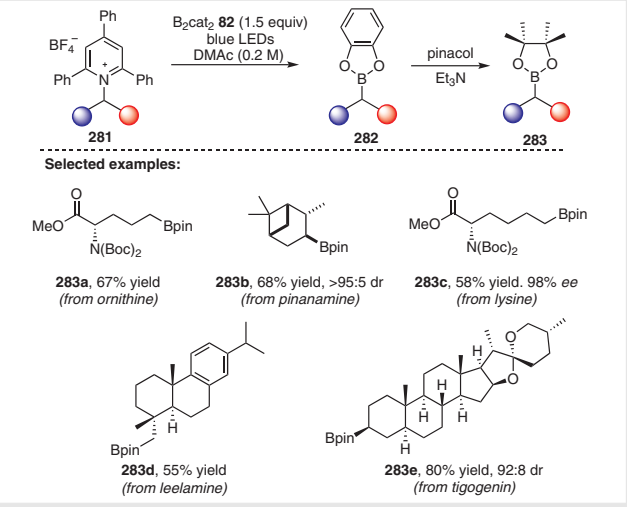

Scheme 114 Photo-driven deaminative borylation reaction

In 2018, the Melchiorre group further expanded the synthetic potential of the EDA photoexcitation strategy by forming an intramolecular EDA complex that was confirmed unambiguously by X-ray single-crystal analysis.[80] An intracomplex SET process upon irradiation with visible light was the key for this transformation, generating radicals to participate in the reaction sustained by a chain propagation mechanism (Scheme 115).

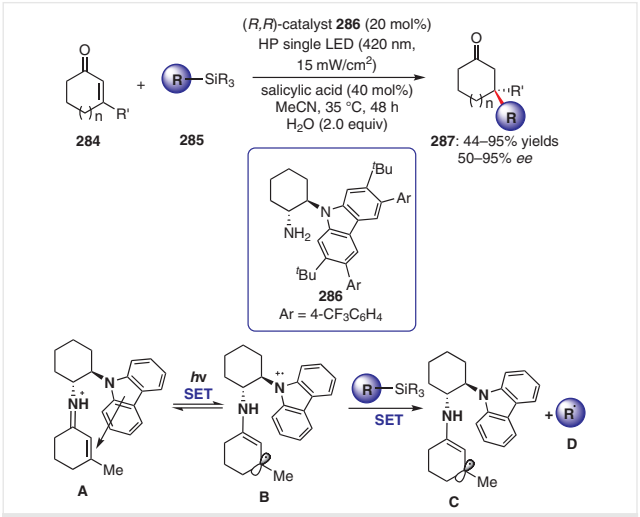

Scheme 115 Enantioselective radical conjugate additions via intramolecular iminium-based EDA complexes

6 Visible Light Photoexcitation of Products

In some cases, the obtained products can also act as photosensitizers in photochemical reactions. In 2015, the Glorius group reported a visible-light-promoted synthesis of indolizines **290** (Scheme 116).[81] The reaction showed great efficiency with α,α,α-trifluorotoluene as the solvent and HMDS as the base under irradiation by blue LEDs. The electronic properties and the position of substituents of brominated pyridines and enol carbamates did not interfere with this transformation. However, the construction of alkyl-substituted indolizines failed under the optimal conditions even in the presence of photocatalyst.

To shed light on the mechanism, UV-visible absorption experiments, Stern–Volmer luminescence quenching experiments, and reaction kinetics experiments were carefully conducted to identify the species responsible for this transformation. After excluding the possibility of product self-replication and EDA complex formation, indolizine **290** was believed to absorb photons in lieu of a photocatalyst. To demonstrate this assumption, indolizine **290** was applied as a photocatalyst in the photoredox-catalyzed reaction of ethyl bromomalonate (**292**) and 1-methyl-1*H*-indole (**291**), successfully delivering the desired product in 45% yield (Scheme 116).

In 2017, Hong and co-workers reported a visible-light-promoted phosphonation of quinolinones with both substrates and products acting as photosensitizers (Scheme 117).[82a] Based on UV-visible absorption spectra and Stern–Volmer quenching experiments, quinolinone **294** was considered a photosensitizer. Interestingly, the reaction rate in-

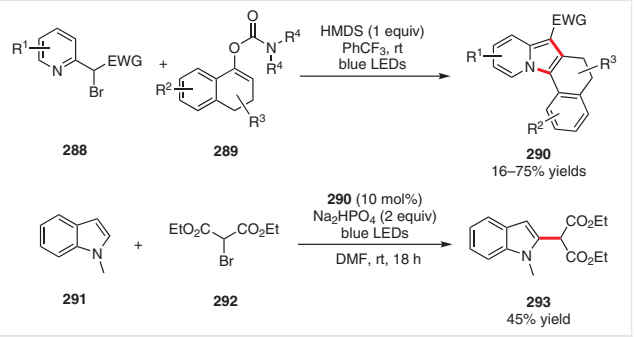

Scheme 116 Visible-light-mediated synthesis of indolizines

creased rapidly once the 3-phosphonylated product **297** was formed. This phenomenon indicated that the product also showed photocatalytic activity. Moreover, the reaction of coumarins also proceeded successfully under the optimized conditions, and bisphosphonated and monophosphonated products were synthesized selectively by easily adjusting conditions.

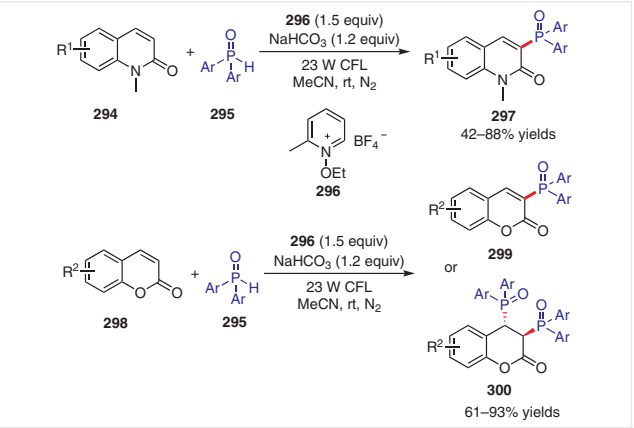

Scheme 117 Visible-light-promoted phosphonation of quinolinones

In 2017, Li, Wang, and co-workers reported a photosensitizer-free oxidative formylation (Scheme 118).[82b] The reaction is spontaneous in an autocatalytic manner in which the substrates and corresponding products act as photosensitizers avoiding use of any external photocatalyst. Based on the results of EPR experiments, the active species $^1O_2$ and $O_2^{\bullet-}$ are assumed to be formed in the reaction system and play important roles in this reaction. In 2018, they further disclosed a protocol for the selective C–H trifluoromethylation of aminoquinoline with both the starting material and product acting as photosensitizers to generate various trifluoromethylated quinolines **305** under green, simple, and mild conditions (Scheme 118).[82c]

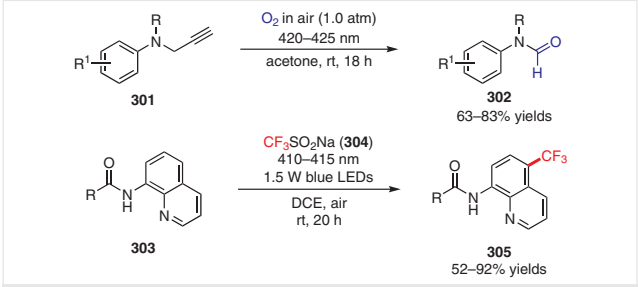

Scheme 118 Visible-light-induced oxidative formylation and C–H trifluoromethylation

7 Conclusion and Outlook

In the past decade, visible-light-driven, photocatalyst-free organic photochemical synthesis has gathered increasing research interests from the synthetic community for its great advantages of user-friendly conditions and the avoidance of precious metals or organic dyes. In this review, we have summarized the important progress by highlighting representative examples in this area according to the photoexcitation modes. We believe that these transformations show an impressive growth in modern organic photochemical synthesis and open a new world of possibilities for constructing various complex architectures using only visible light as a clean reagent and energy source. Notwithstanding the promising progress, the development of additional approaches for visible-light-induced radical initiation and efficient asymmetric transformations is still highly desirable in this research area.

Funding Information

We are grateful to the National Natural Science Foundation of China (Grants No. 21822103, 21820102003, 21772052, 21772053, 21572074, 21472057, and 21602052), the Program of Introducing Talents of Discipline to Universities of China (111 Program) (Grant No. B17019), the Natural Science Foundation of Hubei Province (Grant No. 2017AHB047), and the International Joint Research Center for Intelligent Biosensing Technology and Health, and College Outstanding Young Scientific and Technological Innovation Team of Hubei Province (Grant No. T201718) for support of this research.

References

(1) Ciamician, G. *Science* **1912**, *36*, 385.
(2) (a) Yoon, T. P.; Ischay, M. A.; Du, J. *Nat. Chem.* **2010**, *2*, 527. (b) Schultz, D. M.; Yoon, T. P. *Science* **2014**, *343*, 1239176.
(3) (a) Prier, C. K.; Rankic, D. A.; MacMillan, D. W. C. *Chem. Rev.* **2013**, *113*, 5322. (b) Shaw, M. H.; Twilton, J.; MacMillan, D. W. C. *J. Org. Chem.* **2016**, *81*, 6898.
(4) (a) Nicewicz, D. A.; Nguyen, T. M. *ACS Catal.* **2014**, *4*, 355. (b) Romero, N. A.; Nicewicz, D. A. *Chem. Rev.* **2016**, *116*, 10075.
(5) Lang, X.; Chen, X.; Zhao, J. *Chem. Soc. Rev.* **2014**, *43*, 473.

(6) (a) Nicewicz, D. A.; MacMillan, D. W. C. *Science* **2008**, *322*, 77. For selected reviews, see: (b) Narayanam, J. M. R.; Stephenson, C. R. J. *Chem. Soc. Rev.* **2011**, *40*, 102. (c) Xuan, J.; Xiao, W.-J. *Angew. Chem. Int. Ed.* **2012**, *51*, 6828. (d) Shi, L.; Xia, W. *Chem. Soc. Rev.* **2012**, *41*, 7687. (e) Xi, Y.; Yi, H.; Lei, A. *Org. Biomol. Chem.* **2013**, *11*, 2387. (f) Xuan, J.; Lu, L.-Q.; Chen, J.-R.; Xiao, W.-J. *Eur. J. Org. Chem.* **2013**, *2013*, 6755. (g) Hari, D. P.; König, B. *Angew. Chem. Int. Ed.* **2013**, *52*, 4734. (h) Peña-López, M.; Rosas-Hernndez, A.; Beller, M. *Angew. Chem. Int. Ed.* **2015**, *54*, 5006. (i) Special Issue on Photoredox Catalysis in Organic Chemistry: *Acc. Chem. Res.* **2016**,49 2059. (j) Special Issue on Photochemistry in Organic Synthesis: *Chem. Rev.*116 9629.

(7) Arceo, E.; Jurberg, I. D.; Álvarez-Fernández, A.; Melchiorre, P. *Nat. Chem.* **2013**, *5*, 750.

(8) Arbuj, S. S.; Waghmode, S. B.; Ramaswamy, A. V. *Tetrahedron Lett.* **2007**, *48*, 1411.

(9) Song, L.; Zhang, L.; Luo, S.; Cheng, J.-P. *Chem. Eur. J.* **2014**, *20*, 14231.

(10) (a) Schmidt, V. A.; Quinn, R. K.; Brusoe, A. T.; Alexanian, E. J. *J. Am. Chem. Soc.* **2014**, *136*, 14389. (b) Quinn, R. K.; Könst, Z. A.; Michalak, S. E.; Schmidt, Y.; Szklarski, A. R.; Flores, A. R.; Nam, S.; Horne, D. A.; Vanderwal, C. D.; Alexanian, E. J. *J. Am. Chem. Soc.* **2016**, *138*, 696.

(11) Ni, K.; Meng, L.-G.; Wang, K.; Wang, L. *Org. Lett.* **2018**, *20*, 2245.

(12) Cecere, G.; König, C. M.; Alleva, J. L.; MacMillan, D. W. C. *J. Am. Chem. Soc.* **2013**, *135*, 11521.

(13) Moteki, S. A.; Usui, A.; Selvakumar, S.; Zhang, T.-X.; Maruoka, K. *Angew. Chem. Int. Ed.* **2014**, *53*, 11060.

(14) Jung, J.; Kim, J.; Park, G.; You, Y.; Cho, E. J. *Adv. Synth. Catal.* **2016**, *358*, 74.

(15) Chen, W.-X.; Tao, H.-C.; Huang, W.-H.; Wang, G.-Q.; Li, S.-H.; Cheng, X.; Li, G.-G. *Chem. Eur. J.* **2016**, *22*, 9546.

(16) (a) Buzzetti, L.; Prieto, A.; Roy, S. R.; Melchiorre, P. *Angew. Chem. Int. Ed.* **2017**, *56*, 15039. (b) Goti, G.; Bieszczad, B.; Vega-Peñaloza, A.; Melchiorre, P. *Angew. Chem. Int. Ed.* **2019**, *58*, 1213.

(17) (a) Xu, W.-T.; Huang, B.; Dai, J.-J.; Xu, J.; Xu, H.-J. *Org. Lett.* **2016**, *18*, 3114. (b) Majek, M.; Faltermeier, U.; Dick, B.; Pérez-Ruiz, R.; Jacobi von Wangelin, A. *Chem. Eur. J.* **2015**, *21*, 15496. (c) Liu, W.; Liu, P.; Lv, L.; Li, C.-J. *Angew. Chem. Int. Ed.* **2018**, *57*, 13499.

(18) Zhao, Y.-T.; Huang, B.-B.; Yang, C.; Xia, W.-J. *Org. Lett.* **2016**, *18*, 3326.

(19) Wang, C.-L.; Qiao, J.-Y.; Liu, X.-C.; Song, H.; Sun, Z.-Z.; Chu, W.-Y. *J. Org. Chem.* **2018**, *83*, 1422.

(20) (a) Li, M.-M.; Wei, Y.; Liu, J.; Chen, H.-W.; Lu, L.-Q.; Xiao, W.-J. *J. Am. Chem. Soc.* **2017**, *139*, 14707. (b) Wei, Y.; Lu, L.-Q.; Li, T.-R.; Feng, B.; Wang, Q.; Xiao, W.-J.; Alper, H. *Angew. Chem. Int. Ed.* **2016**, *55*, 2200. (c) Wei, Y.; Liu, S.; Li, M.-M.; Li, Y.; Lan, Y.; Lu, L.-Q.; Xiao, W.-J. *J. Am. Chem. Soc.* **2019**, *141*, 133. (d) Liu, J.; Li, M.-M.; Qu, B.-L.; Lu, L.-Q.; Xiao, W.-J. *Chem. Commun.* **2019**, *55*, 2031. (e) Liu, D.; Ding, W.; Zhou, Q.-Q.; Wei, Y.; Lu, L.-Q.; Xiao, W.-J. *Org. Lett.* **2018**, *20*, 7278.

(21) Ishida, K.; Tobita, F.; Kusama, H. *Chem. Eur. J.* **2018**, *24*, 543.

(22) (a) Zhang, H.-J.; Becker, P.; Huang, H.; Pirwerdjan, R.; Pan, F.-F.; Bolm, C. *Adv. Synth. Catal.* **2012**, *354*, 2157. (b) Becker, P.; Priebbenow, D. L.; Zhang, H.-J.; Pirwerdjan, R.; Bolm, C. *J. Org. Chem.* **2014**, *79*, 814.

(23) Liu, P.; Liu, W.-B.; Li, C.-J. *J. Am. Chem. Soc.* **2017**, *139*, 14315.

(24) Shi, Q.; Li, P.-H.; Zhang, Y.; Wang, L. *Org. Chem. Front.* **2017**, *4*, 1322.

(25) Sahoo, H.; Mandal, A.; Dana, S.; Baidya, M. *Adv. Synth. Catal.* **2018**, *360*, 1099.

(26) (a) Cheng, Y.; Mück-Lichtenfeld, C.; Studer, A. *J. Am. Chem. Soc.* **2018**, *140*, 6221. (b) Cheng, Y.; Mück-Lichtenfeld, C.; Studer, A. *Angew. Chem. Int. Ed.* **2018**, *57*, 16832.

(27) Kischkewitz, M.; Gerleve, C.; Studer, A. *Org. Lett.* **2018**, *20*, 3666.

(28) Wang, M.-Y.; Cao, Y.; Liu, X.; Wang, N.; He, L.-N.; Li, S.-H. *Green Chem.* **2017**, *19*, 1240.

(29) (a) Southgate, E. H.; Pospech, J.; Fu, J.; Holycross, D. R.; Sarlah, D. *Nat. Chem.* **2016**, *8*, 922. (b) Okumura, M.; Shved, A. S.; Sarlah, D. *J. Am. Chem. Soc.* **2017**, *139*, 17787. (c) Hernandez, L. W.; Pospech, J.; Kloeckner, U.; Bingham, T. W.; Sarlah, D. *J. Am. Chem. Soc.* **2017**, *139*, 15656. (d) Hernandez, L. W.; Klöckner, U.; Pospech, J.; Hauss, L.; Sarlah, D. *J. Am. Chem. Soc.* **2018**, *140*, 4503. (e) Wertjes, W. C.; Okumura, M.; Sarlah, D. *J. Am. Chem. Soc.* **2019**, *141*, 163.

(30) Leow, D.-S.; Chen, Y.-H.; Hung, T.-H.; Su, Y.; Lin, Y.-Z. *Eur. J. Org. Chem.* **2014**, *2014*, 7347.

(31) Park, S.; Jung, J.; Cho, E.-J. *Eur. J. Org. Chem.* **2014**, *2014*, 4148.

(32) (a) Tan, H.; Li, H.-J.; Ji, W.-Q.; Wang, L. *Angew. Chem. Int. Ed.* **2015**, *54*, 8374. (b) Ji, W.-Q.; Tan, H.; Wang, M.; Li, P.-H.; Wang, L. *Chem. Commun.* **2016**, *52*, 1462.

(33) (a) Pratsch, G.; Lackner, G. L.; Overman, L. E. *J. Org. Chem.* **2015**, *80*, 6025. (b) Jin, Y.-H.; Yang, H.-J.; Fu, H. *Chem. Commun.* **2016**, *52*, 12909. (c) Jin, Y.-H.; Yang, H.-J.; Fu, H. *Org. Lett.* **2016**, *18*, 6400.

(34) (a) Fawcett, A.; Pradeilles, J.; Wang, Y.; Mutsuga, T.; Myers, E. L.; Aggarwal, V. K. *Science* **2017**, *357*, 283. (b) Candish, L.; Teders, M.; Glorius, F. *J. Am. Chem. Soc.* **2017**, *139*, 7440.

(35) (a) Usami, K.; Nagasawa, Y.; Yamaguchi, E.; Tada, N.; Itoh, A. *Org. Lett.* **2016**, *18*, 8. (b) Qian, P.; Du, B.-N.; Song, R.-C.; Wu, X.-D.; Mei, H.-B.; Han, J.-L.; Pan, Y. *J. Org. Chem.* **2016**, *81*, 6546.

(36) Yamaguchi, E.; Sudo, Y.; Tada, N.; Itoh, A. *Adv. Synth. Catal.* **2016**, *358*, 3191.

(37) Sudo, Y.; Yamaguchi, E.; Itoh, A. *Org. Lett.* **2017**, *19*, 1610.

(38) Xu, Z.; Gao, L.; Wang, L.-L.; Gong, M.-W.; Wang, W.-F.; Yuan, R.-S. *ACS Catal.* **2015**, *5*, 45.

(39) Zhao, M.-D.; Lu, W.-J. *Org. Lett.* **2017**, *19*, 4560.

(40) Huang, L.; Rudolph, M.; Rominger, F.; Hashmi, A. S. K. *Angew. Chem. Int. Ed.* **2016**, *55*, 4808.

(41) Witzel, S.; Xie, J.; Rudolph, M.; Hashmi, A. S. K. *Adv. Synth. Catal.* **2017**, *359*, 1522.

(42) Liang, Y.-F.; Steinbock, R.; Yang, L.; Ackermann, L. *Angew. Chem. Int. Ed.* **2018**, *57*, 10625.

(43) Zhang, L.-L.; Zhang, G.-T.; Li, Y.-L.; Wang, S.-C.; Lei, A. *Chem. Commun.* **2018**, *54*, 5744.

(44) Silvi, M.; Arceo, E.; Jurberg, I. D.; Cassani, C.; Melchiorre, P. *J. Am. Chem. Soc.* **2015**, *137*, 6120.

(45) Silvi, M.; Verrier, C.; Rey, Y. P.; Buzzetti, L.; Melchiorre, P. *Nat. Chem.* **2017**, *9*, 868.

(46) Bonilla, P.; Rey, Y. P.; Holden, C. M.; Melchiorre, P. *Angew. Chem. Int. Ed.* **2018**, *57*, 12819.

(47) Mazzarella, D.; Crisenza, G. E. M.; Melchiorre, P. *J. Am. Chem. Soc.* **2018**, *140*, 8439.

(48) Woźniak, Ł.; Magagnano, G.; Melchiorre, P. *Angew. Chem. Int. Ed.* **2018**, *57*, 1068.

(49) Schweitzer-Chaput, B.; Horwitz, M. A.; de Pedro Beato, E.; Melchiorre, P. *Nat. Chem.* **2019**, *11*, 129.

(50) Filippini, G.; Nappi, M.; Melchiorre, P. *Tetrahedron* **2015**, *71*, 4535.

(51) Wu, X.-X.; Zhang, H.; Tang, N.-N.; Wu, Z.; Wang, D.-P.; Ji, M.-S.; Xu, Y.; Wang, M.; Zhu, C. *Nat. Commun.* **2018**, *9*, 3343.

(52) Kainz, Q. M.; Matier, C. D.; Bartoszewicz, A.; Zultanski, S. L.; Peters, J. C.; Fu, G. C. *Science* **2016**, *351*, 681.

(53) (a) Sagadevana, A.; Hwang, K. C. *Adv. Synth. Catal.* **2012**, *354*, 3421. (b) Sagadevan, A.; Ragupathi, A.; Hwang, K. C. *Photochem. Photobiol. Sci.* **2013**, *12*, 2110. (c) Sagadevan, A.; Ragupathi, A.; Hwang, K. C. *Angew. Chem. Int. Ed.* **2015**, *54*, 13896. (d) Sagadevan, A.; Ragupathi, A.; Lin, C.-C.; Hwu, J. R.; Hwang, K. C. *Green Chem.* **2015**, *17*, 1113. (e) Ragupathi, A.; Sagadevan, A.; Lin, C.-C.; Hwu, J. R.; Hwang, K. C. *Chem. Commun.* **2016**, *52*, 11756. (f) Sagadevan, A.; Charpe, V. P.; Hwang, K. C. *Catal. Sci. Technol.* **2016**, *6*, 7688. (g) Sagadevan, A.; Lyu, P.-C.; Hwang, K. C. *Green Chem.* **2016**, *18*, 4526. (h) Sagadevan, A.; Charpe, V. P.; Ragupathi, A.; Hwang, K. C. *J. Am. Chem. Soc.* **2017**, *139*, 2896.

(54) Lei, W.-L.; Wang, T.; Feng, K.-W.; Wu, L.-Z.; Liu, Q. *ACS Catal.* **2017**, *7*, 7941.

(55) Meng, Q.-Y.; Gao, X.-W.; Lei, T.; Liu, Z.; Zhan, F.; Li, Z.-J.; Zhong, J.-J.; Xiao, H.-Y.; Feng, K.; Chen, B.; Tao, Y.; Tung, C.-H.; Wu, L.-Z. *Sci. Adv.* **2017**, *3*, e1700666.

(56) Cai, S.-Y.; Yang, K.; Wang, D. Z. *Org. Lett.* **2014**, *16*, 2606.

(57) Zhang, T.; Meng, Y.-G.; Lu, J.-Y.; Yang, Y.-T.; Li, G.-Q.; Zhu, C.-Y. *Adv. Synth. Catal.* **2018**, *360*, 3063.

(58) Yuan, J.; To, W.-P.; Zhang, Z.-Y.; Yue, C.-D.; Meng, S.-X.; Chen, J.; Liu, Y.-G.; Yu, G.-A.; Che, C.-M. *Org. Lett.* **2018**, *20*, 7816.

(59) Pham, P. V.; Nagib, D. A.; MacMillan, D. W. C. *Angew. Chem. Int. Ed.* **2011**, *50*, 6119.

(60) Tobisu, M.; Furukawa, T.; Chatani, N. *Chem. Lett.* **2013**, *42*, 1203.

(61) (a) Kandukuri, S. R.; Bahamonde, A.; Chatterjee, I.; Jurberg, I. D.; Escudero-Adan, E. C.; Melchiorre, P. *Angew. Chem. Int. Ed.* **2015**, *54*, 1485. (b) Zhu, M.; Zhou, K.; Zhang, X.; You, S. L. *Org. Lett.* **2018**, *20*, 4379.

(62) da Silva, G. P.; Ali, A.; da Silva, R. C.; Jiang, H.; Paixão, M. W. *Chem. Commun.* **2015**, *51*, 15110.

(63) Franz, J. F.; Kraus, W. B.; Zeitler, K. *Chem. Commun.* **2015**, *51*, 8280.

(64) (a) Davies, J.; Booth, S. G.; Essafi, S.; Dryfe, R. A. W.; Leonori, D. *Angew. Chem. Int. Ed.* **2015**, *54*, 14017. (b) Li, J. J.; Zhang, P. X.; Jiang, M.; Yang, H. J.; Zhao, Y. F.; Fu, H. *Org. Lett.* **2017**, *19*, 1994. (c) Li, Y. W.; Mao, R. Y.; Wu, J. *Org. Lett.* **2017**, *19*, 4472. (d) Mao, R. Y.; Yuan, Z.; Li, Y. W.; Wu, J. *Chem. Eur. J.* **2017**, *23*, 8176.

(65) (a) Liu, N. W.; Chen, Z. K.; Herbert, A.; Ren, H. J.; Manolikakes, G. *Eur. J. Org. Chem.* **2018**, *2018*, 5725. (b) Lecroq, W.; Bazille, P.; Morlet-Savary, F.; Breugst, M.; Lalevée, J.; Gaumont, A. C.; Lakhdar, S. *Org. Lett.* **2018**, *20*, 4164.

(66) Spell, M. L.; Deveaux, K.; Bresnahan, C. G.; Bernard, B. L.; Sheffield, W.; Kumar, R.; Ragains, J. R. *Angew. Chem. Int. Ed.* **2016**, *55*, 6515.

(67) Supranovich, V. I.; Levin, V. V.; Struchkova, M. I.; Korlyukov, A. A.; Dilman, A. D. *Org. Lett.* **2017**, *19*, 3215.

(68) (a) Sun, X. Y.; Wang, W. M.; Li, Y. L.; Ma, J.; Yu, S. Y. *Org. Lett.* **2016**, *18*, 4638. (b) Tang, X. J.; Studer, A. *Chem. Sci.* **2017**, *8*, 6888.

(69) Marzo, L.; Wang, S.; König, B. *Org. Lett.* **2017**, *19*, 5976.

(70) Zhang, J.; Li, Y.; Xu, R. Y.; Chen, Y. Y. *Angew. Chem. Int. Ed.* **2017**, *56*, 12619.

(71) Arceo, E.; Bahamonde, A.; Bergonzini, G.; Melchiorre, P. *Chem. Sci.* **2014**, *5*, 2438.

(72) Nappi, M.; Bergonzini, G.; Melchiorre, P. *Angew. Chem. Int. Ed.* **2014**, *53*, 4921.

(73) Woźniak, Ł.; Murphy, J. J.; Melchiorre, P. *J. Am. Chem. Soc.* **2015**, *137*, 5678.

(74) Gao, L.; Chang, B.; Qiu, W. Z.; Wang, L.; Fu, X. Z.; Yuan, R. S. *Adv. Synth. Catal.* **2016**, *358*, 1202.

(75) Liu, Y.-Y.; Yu, X.-Y.; Chen, J.-R.; Qiao, M.-M.; Qi, X.-T.; Shi, D.-Q.; Xiao, W.-J. *Angew. Chem. Int. Ed.* **2017**, *56*, 9527.

(76) (a) Liu, B.; Lim, C.-H.; Miyake, G. M. *J. Am. Chem. Soc.* **2017**, *139*, 13616. (b) Liu, B.; Lim, C.-H.; Miyake, G. M. *J. Am. Chem. Soc.* **2018**, *140*, 12829.

(77) Li, Y.; Miao, T.; Li, P. H.; Wang, L. *Org. Lett.* **2018**, *20*, 1735.

(78) Guo, W.; Zhao, M. M.; Tan, W.; Zheng, L.; Tao, K. L.; Liu, L. X.; Wang, X. Y.; Chen, D. L.; Fan, X. L. *J. Org. Chem.* **2018**, *83*, 1402.

(79) Wu, J. J.; He, L.; Noble, A.; Aggarwal, V. K. *J. Am. Chem. Soc.* **2018**, *140*, 10700.

(80) Cao, Z. Y.; Ghosh, T.; Melchiorre, P. *Nat. Commun.* **2018**, *9*, 3274.

(81) Sahoo, B.; Hopkinson, M. N.; Glorius, F. *Angew. Chem. Int. Ed.* **2015**, *54*, 15545.

(82) (a) Kim, I.; Min, M.; Kang, D.; Kim, K.; Hong, S. *Org. Lett.* **2017**, *19*, 1394. (b) Ji, W. Q.; Li, P. H.; Yang, S.; Wang, L. *Chem. Commun.* **2017**, *53*, 8482. (c) Zhao, L. L.; Li, P. H.; Xie, X. Y.; Wang, L. *Org. Chem. Front.* **2018**, *5*, 1689.